QUT

QUEENSLAND UNIVERSITY OF TECHNOLOGY

SCHOOL OF PHYSICAL AND CHEMICAL SCIENCES

INORGANIC MATERIALS RESEARCH GROUP

Synthesis and Modifications of Metal Oxide Nanostructures and Their Applications

Submitted by Zhanfeng Zheng, under the supervision of Prof. Huaiyong Zhu and Prof. Ray R. Frost, to the School of Physical and Chemical Sciences, Queensland University of Technology, in partial fulfilment of the requirements of the degree of Doctor of Philosophy.

2009

KEYWORDS

Metal oxide, nanostructure, nanofibre, nanotube, hydrothermal, titanate, niobate, TiO_2, anatase, $TiO_2(B)$, mixed-phase, interface, supported gold catalyst, photocatalysis, charge separation, catalytic oxidation, surface chemistry, surface OH groups, absorbent, nanofilter

ABSTRACT

Transition metal oxides are functional materials that have advanced applications in many areas, because of their diverse properties (optical, electrical, magnetic, etc.), hardness, thermal stability and chemical resistance. Novel applications of the nanostructures of these oxides are attracting significant interest as new synthesis methods are developed and new structures are reported. Hydrothermal synthesis is an effective process to prepare various delicate structures of metal oxides on the scales from a few to tens of nanometres, specifically, the highly dispersed intermediate structures which are hardly obtained through pyro-synthesis. In this thesis, a range of new metal oxide (stable and metastable titanate, niobate) nanostructures, namely nanotubes and nanofibres, were synthesised via a hydrothermal process. Further structure modifications were conducted and potential applications in catalysis, photocatalysis, adsorption and construction of ceramic membrane were studied.

The morphology evolution during the hydrothermal reaction between Nb_2O_5 particles and concentrated NaOH was monitored. The study demonstrates that by optimising the reaction parameters (temperature, amount of reactants), one can obtain a variety of nanostructured solids, from intermediate phases niobate bars and fibres to the stable phase cubes. Trititanate ($Na_2Ti_3O_7$) nanofibres and nanotubes were obtained by the hydrothermal reaction between TiO_2 powders or a titanium compound (e.g. $TiOSO_4 \cdot xH_2O$) and concentrated NaOH solution by controlling the reaction temperature and NaOH concentration. The trititanate possesses a layered structure, and the Na ions that exist between the negative charged titanate layers are exchangeable with other metal ions or H^+ ions. The ion-exchange has crucial influence on the phase transition of the exchanged products. The exchange of the sodium ions in the titanate with H^+ ions yields protonated titanate (H-titanate) and subsequent phase transformation of the H-titanate enable various TiO_2 structures with

retained morphology. H-titanate, either nanofibres or tubes, can be converted to pure TiO$_2$(B), pure anatase, mixed TiO$_2$(B) and anatase phases by controlled calcination and by a two-step process of acid-treatment and subsequent calcination. While the controlled calcination of the sodium titanate yield new titanate structures (metastable titanate with formula Na$_{1.5}$H$_{0.5}$Ti$_3$O$_7$, with retained fibril morphology) that can be used for removal of radioactive ions and heavy metal ions from water. The structures and morphologies of the metal oxides were characterised by advanced techniques.

Titania nanofibres of mixed anatase and TiO$_2$(B) phases, pure anatase and pure TiO$_2$(B) were obtained by calcining H-titanate nanofibres at different temperatures between 300 and 700 °C. The fibril morphology was retained after calcination, which is suitable for transmission electron microscopy (TEM) analysis. It has been found by TEM analysis that in mixed-phase structure the interfaces between anatase and TiO$_2$(B) phases are not random contacts between the engaged crystals of the two phases, but form from the well matched lattice planes of the two phases. For instance, (101) planes in anatase and (101) planes of TiO$_2$(B) are similar in d spaces (~0.18 nm), and they join together to form a stable interface. The interfaces between the two phases act as an one-way valve that permit the transfer of photogenerated charge from anatase to TiO$_2$(B). This reduces the recombination of photogenerated electrons and holes in anatase, enhancing the activity for photocatalytic oxidation. Therefore, the mixed-phase nanofibres exhibited higher photocatalytic activity for degradation of sulforhodamine B (SRB) dye under ultraviolet (UV) light than the nanofibres of either pure phase alone, or the mechanical mixtures (which have no interfaces) of the two pure phase nanofibres with a similar phase composition. This verifies the theory that the difference between the conduction band edges of the two phases may result in charge transfer from one phase to the other, which results in effectively the photogenerated charge separation and thus facilitates the redox reaction involving these charges. Such an interface structure facilitates charge transfer crossing the interfaces. The knowledge acquired in this study is important not only for design of

efficient TiO$_2$ photocatalysts but also for understanding the photocatalysis process. Moreover, the fibril titania photocatalysts are of great advantage when they are separated from a liquid for reuse by filtration, sedimentation, or centrifugation, compared to nanoparticles of the same scale.

The surface structure of TiO$_2$ also plays a significant role in catalysis and photocatalysis. Four types of large surface area TiO$_2$ nanotubes with different phase compositions (labelled as NTA, NTBA, NTMA and NTM) were synthesised from calcination and acid treatment of the H-titanate nanotubes. Using the *in situ* FTIR emission spectrescopy (IES), desorption and re-adsorption process of surface OH-groups on oxide surface can be trailed. In this work, the surface OH-group regeneration ability of the TiO$_2$ nanotubes was investigated. The ability of the four samples distinctively different, having the order: NTA > NTBA > NTMA > NTM. The same order was observed for the catalytic when the samples served as photocatalysts for the decomposition of synthetic dye SRB under UV light, as the supports of gold (Au) catalysts (where gold particles were loaded by a colloid-based method) for photodecomposition of formaldehyde under visible light and for catalytic oxidation of CO at low temperatures. Therefore, the ability of TiO$_2$ nanotubes to generate surface OH-groups is an indicator of the catalytic activity. The reason behind the correlation is that the oxygen vacancies at bridging O^{2-} sites of TiO$_2$ surface can generate surface OH-groups and these groups facilitate adsorption and activation of O$_2$ molecules, which is the key step of the oxidation reactions. The structure of the oxygen vacancies at bridging O^{2-} sites is proposed. Also a new mechanism for the photocatalytic formaldehyde decomposition with the Au-TiO$_2$ catalysts is proposed: The visible light absorbed by the gold nanoparticles, due to surface plasmon resonance effect, induces transition of the 6*sp* electrons of gold to high energy levels. These energetic electrons can migrate to the conduction band of TiO$_2$ and are seized by oxygen molecules. Meanwhile, the gold nanoparticles capture electrons from the formaldehyde molecules adsorbed on them because of gold's high electronegativity.

O_2 adsorbed on the TiO_2 supports surface are the major electron acceptor. The more O_2 adsorbed, the higher the oxidation activity of the photocatalyst will exhibit.

The last part of this thesis demonstrates two innovative applications of the titanate nanostructures. Firstly, trititanate and metastable titanate ($Na_{1.5}H_{0.5}Ti_3O_7$) nanofibres are used as intelligent absorbents for removal of radioactive cations and heavy metal ions, utilizing the properties of the ion exchange ability, deformable layered structure, and fibril morphology. Environmental contamination with radioactive ions and heavy metal ions can cause a serious threat to the health of a large part of the population. Treatment of the wastes is needed to produce a waste product suitable for long-term storage and disposal. The ion-exchange ability of layered titanate structure permitted adsorption of bivalence toxic cations (Sr^{2+}, Ra^{2+}, Pb^{2+}) from aqueous solution. More importantly, the adsorption is irreversible, due to the deformation of the structure induced by the strong interaction between the adsorbed bivalent cations and negatively charged TiO_6 octahedra, and results in permanent entrapment of the toxic bivalent cations in the fibres so that the toxic ions can be safely deposited. Compared to conventional clay and zeolite sorbents, the fibril absorbents are of great advantage as they can be readily dispersed into and separated from a liquid.

Secondly, new generation membranes were constructed by using large titanate and small γ-alumina nanofibres as intermediate and top layers, respectively, on a porous alumina substrate via a spin-coating process. Compared to conventional ceramic membranes constructed by spherical particles, the ceramic membrane constructed by the fibres permits high flux because of the large porosity of their separation layers. The voids in the separation layer determine the selectivity and flux of a separation membrane. When the sizes of the voids are similar (which means a similar selectivity of the separation layer), the flux passing through the membrane increases with the volume of the voids which are filtration passages. For the ideal and simplest texture, a mesh constructed with the nanofibres 10 nm thick and having a uniform pore size of

60 nm, the porosity is greater than 73.5 %. In contrast, the porosity of the separation layer that possesses the same pore size but is constructed with metal oxide spherical particles, as in conventional ceramic membranes, is 36% or less. The membrane constructed by titanate nanofibres and a layer of randomly oriented alumina nanofibres was able to filter out 96.8% of latex spheres of 60 nm size, while maintaining a high flux rate between 600 and 900 Lm^{-2} h^{-1}, more than 15 times higher than the conventional membrane reported in the most recent study.

LIST OF PUBLICATIONS

Journal publications:

1. **Zhanfeng Zheng**, Jaclyn Teo, Xi Chen, Hongwei Liu, Yong Yuan, Eric R. Waclawik, Ziyi Zhong,* and Huaiyong Zhu,* "Correlation of the Catalytic Activity for Oxidation Taking Place on Various TiO_2 Surfaces with Surface OH Groups and Surface Oxygen Vacancies" *Chem. Euro. J.* in press, 2009 **[Impact Factor(IF) in 2008: 5.454]**

2. **Zhanfeng Zheng**, Hongwei Liu, Jianping Ye, Xueping Gao, Jincai Zhao, Eric R. Waclawik, Huaiyong Zhu,* "Structure and Contribution to Photocatalytic Activity of the Interfaces in Nanofibers with Mixed Anatase and $TiO_2(B)$ Phases", *J. Mol. Catal. A* **316**,75-82 (2010) **[IF: 2.814]**

3. Hongwei Liu, Dongjiang Yang, **Zhanfeng Zheng**, Eric Waclawik, Xuebin Ke, Huaiyong Zhu,* Ray Frost, "A Raman spectroscopic and TEM study on the structural evolution of $Na_2Ti_3O_7$ during the transition to $Na_2Ti_6O_{13}$", *J. Raman Spectrosc.* (in press) **[IF: 3.526]**

4. Dongjing Yang, Hongwei Liu, **Zhanfeng Zheng**, Yong Yuan, Jincai Zhao, Eric R. Waclawik, Xuebin Ke, Huaiyong Zhu. "An Efficient Photocatalyst Structure, $TiO_2(B)$ Nanofibers with a Shell of Anatase Nanocrystals", *J. Am. Chem. Soc.* in press, 2009 **[IF: 8.091]**

5. Huaiyong Zhu*, Xi Chen, **Zhanfeng Zheng**, Xuebin Ke, Esa Jaatinen, Jincai Zhao,Cheng Guo, Tengfeng Xie, Dejun Wang, "Mechanism of supported gold nanoparticles as photocatalysts under ultraviolet and visible light irradiation", *Chem. Commun.* (in press)**[IF: 5.34]**

6. Dongjiang Yang, **Zhanfeng Zheng**, Huaiyong Zhu*, Hongwei Liu, Xueping Gao, "Titanate Nanofibers as Intelligent Absorbents for the Removal of Radioactive Ions from Water", *Adv. Mater.* **20,** 2777-2781 (2008). **[IF: 8.191]**

7. Dongjiang Yang, **Zhanfeng Zheng**, Hongwei Liu, Huaiyong Zhu*, Xuebin Ke, Yao Xu, Dong Wu, Yuhan Sun, "Layered Titanate Nanofibers as Efficient

Absorbents for Removal of Toxic Radioactive and Heavy Metal Ions from Water", *J Phys. Chem. B* **112,** 16275-16280 (2008). **[IF: 4.189]**

8. Xuebin Ke, **Zhanfeng Zheng**, Hongwei Liu, Huaiyong Zhu*, Xueping Gao, Lixiong Zhang, Nanping Xu, Huanting Wang, Huijun Zhao, Jeffery Shi, Kyle R. Ratinac, *"*High-Flux Ceramic Membranes with a Nanomesh of Metal Oxide Nanofibers", *J. Phys. Chem. B* 112,5000-5006 (2008). **[IF: 4.189]**

9. Xi Chen, Huaiyong Zhu*, Jincai Zhao, **Zhanfeng Zheng**, Xueping Gao, *"*Visible-Light-Driven Oxidation of Organic Contaminants in Air with Gold Nanoparticle Catalysts on Oxide Supports", *Angew. Chem. Int. Ed.* 120, 5433-5436 (2008). **[IF: 10.879]**

10. Xuebin Ke, Huaiyong Zhu*, Xueping Gao, Jiangwen Liu, **Zhanfeng Zheng**, "High-performance ceramic membranes with a separation layer of metal oxide nanofibers", *Adv. Mater.* 19,785-790 (2007). **[IF: 8.191]**

11. Pu Xu*, Xiaoming Wen, **Zhanfeng Zheng**, Guy Cox, Huaiyong Zhu, "Two-photon optical characteristics of zinc oxide in bulk, low dimensional and nanoforms", *J. Lumin.* 126,641-643 (2007). **[IF: 1.628]**

12. Huaiyong Zhu*, **Zhanfeng Zheng**, Xueping Gao, Yining Huang, Z. M. Yan, Jin Zou, Hongming Yin, Qingdi Zou, Scott H. Kable, Jincai Zhao, Yunfei Xi, Wayde N. Martens, Ray L. Frost, *"*Structural evolution in a hydrothermal reaction between Nb_2O_5 and NaOH solution: From Nb_2O_5 grains to microporous $Na_2Nb_2O_6 \cdot 2/3H_2O$ fibers and $NaNbO_3$ cubes", *J. Am. Chem. Soc.* 128, 2373-2384 (2006). **[IF: 8.091]**

Conference presentation:

13. **Zhanfeng Zheng**, Hongwei Liu, Huaiyong Zhu*, "*Photocatalytic Activity and Interface Structure of Nanofibres with Mixed Anatase and TiO2(B) Phases"* 16th **International Conference on Composites or Nano Engineering (ICCE-16)**, Kunming, China, July 20-26, 2008.

DECLARATION OF ORIGINAL AUTHORSHIP

The work contained in this thesis has not been previously submitted to meet requirements for an award at this or any other education institution. To the best of my knowledge and belief, the thesis contains no material previously published or written by another person except where due reference is made.

Signed:_____Z. F. Zheng_____

(Zhanfeng ZHENG)

Date:_____08/11/2009_____

ACKNOWLEDGEMENTS

TABLE OF CONTENTS

TABLE OF FIGURES

LIST OF ABBREVIATIONS

1D	One dimensional
AFM	Atomic force microscopy
ALD	Atomic layer deposition
BET	Brunauer-Emmett-Teller
CP	Co-precipitation
CVD	Chemical vapour deposition
DFT	Density functional theory
DP	Deposition-precipitation
EDP	Electron diffraction pattern
EDS	Energy dispersive X-Ray spectroscopy
GC	Gas chromatography
ICP	Inductively coupled plasma
IES	FT-IR emission spectroscopy
IP	Impregnation
LROF	Layers of randomly oriented fibres
MS	Mass spectrometry
NMR	Nuclear magnetic resonance spectroscopy
PL	Photoluminescence spectroscopy
PLD	Pulsed laser deposition
SEM	Scanning electron microscopy
SOMS	Sandia octahedral molecular sieves
SPM	Scanning probe microscopy
SPR	Surface plasmon resonance
SRB	Sulforhodamine B
STM	Scanning tunnelling microscopy

TEM	Transmission electron microscopy
TG	Thermogravimetric analysis
TOF	Turnover frequency
TPD	Temperature programmed desorption
UV-vis	Ultraviolet-visible spectra
VLS	Vapour-Liquid-Solid
VOCs	Volatile organic compounds
XPS	X-ray photoelectron spectroscopy
XRD	X-ray diffraction

CHAPTER 1. INTRODUCTION AND LITERATURE REVIEW

1.1 Introduction

Metal oxides play a very important role in many areas of chemistry, physics, and materials science.[1-4] The metal elements can form a large diversity of oxide compounds by employing various synthesis techniques. They exhibit metallic, semiconductor, or insulator character due to the electronic structure difference. The variety of attributes of oxides enable the wide applications in the fabrication of microelectronic circuits, sensors, piezoelectric devices, fuel cells, coatings against corrosion, and as catalysts. For example, almost all catalysts involve an oxide as active phase, promoter(or support) which allows the active components to disperse on. In the chemical and petrochemical industries, products worth billions of dollars are generated every year through processes that use oxide and metal/oxide catalysts. For the control of environmental pollution, catalysts or sorbents that contain oxides are employed to remove the CO, NO_x, and SO_x species formed during the combustion of fossil-derived fuels.[5] Furthermore, the most active areas of the semiconductor industry involve the use of oxides. Thus, most of the chips used in computers contain an oxide component. Till now, there are still many potential applications of these materials under continuous investigation and new synthesis methods being developed.[6] To exploit new applications metal oxide materials is one of the mean purposes of inorganic chemist.

Ever since the discovery of carbon nanotubes by Iijima,[7] the synthesis, characterisation and applications of the inorganic nanostructured materials have drawn great interest.[8-10] Metal oxide nanomaterials have attracted great interest because of many unique properties linked to the nanometre size of the particles.[8-12]

4

Particle size is expected to influence the properties mainly in two aspects. The first one is the change in structural characteristics, such as the lattice symmetry and cell parameters. Bulk oxides are usually robust and stable systems with well-defined crystallographic structures. The other one is the presence of under-coordinated atoms (like corners or edges) or O vacancies in an oxide nanoparticle. These under-coordinated atoms or O vacancies should produce atomic arrangements different from that in the bulk material as well as occupied electronic states located above the valence band of the corresponding bulk material, enhancing the chemical activity of the system. These properties of nanostructured oxides lead to the wide industrial applications as sorbents, sensors, ceramic materials, photo-devices, and catalysts for reducing environmental pollution, transforming hydrocarbons, and producing H_2.[1, 4] To prepare these nanomaterials, novel synthesis procedures have been developed that can be described as physical and chemical methods. In general, they use top-down and bottom-up fabrication approaches, which involve liquid–solid or gas–solid transformations.[9-16] Moreover, these materials can be further functionalised by surface and structure modification. The good thermal and chemical stability of these inorganic materials enable them to be widely used.

1.2 Basic Concepts - Nanotechnology and Nanomaterials

In general, nanotechnology can be understood as a technology of design, fabrication and applications of nanostructures and nanomaterials, as well as fundamental understanding of physical properties and phenomena of nanomaterials and nanostructures.[13, 14] Nanomaterials, compared to bulk materials, have the scales ranging from individual atoms or molecules to submicron dimensions at least in one dimension. Nanomaterials and nanotechnology have found the significant applications in physical, chemical and biological systems. The importance of nanotechnology was pointed out by Feynman at the annual meeting of the American Physical Society in 1959, in the classic science lecture entitled ''There is plenty of

room at the bottom''. Since 1980s, many inventions and discoveries in the fabrication of nano-objects have been developed. The discovery of novel materials, processes, and phenomena at the nanoscale, as well as the development of new experimental and theoretical techniques for research provide plenty of new opportunities for the development of innovative nanostructured materials. Nanostructured materials can be made with unique nanostructures and properties. This field is expected to open new venues in science and technology.

1.2.1 Size Effects
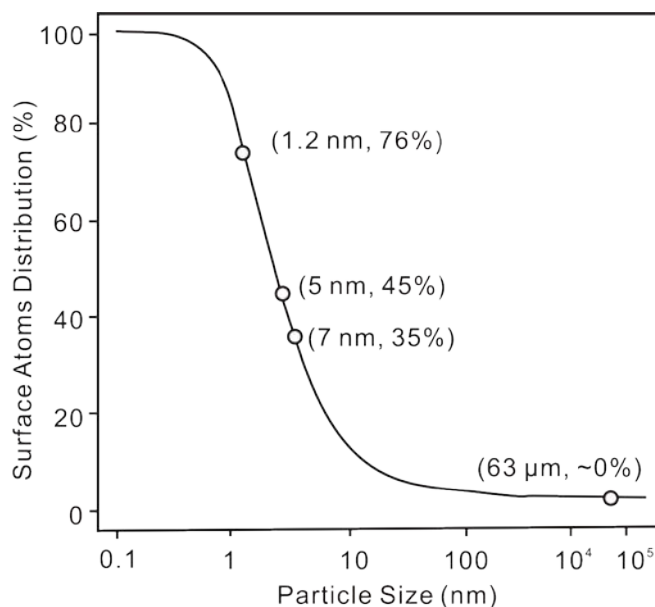
Figure 1. The percentage of surface atoms changing with the palladium cluster diameter. Adapted from reference (ref) 15.

The main apparent difference between bulk material and nanomaterial lays on the size difference. With the decrease of the particle size, distinctly different properties of nanomaterial emerge compared to its bulk structure. This makes the nanomaterials a class of novel materials with tremendous new applications. The terminal, size effects, is used to describe the properties change accompanied with particle size change. The effects determined by size pertain to the evolution of structural, thermodynamic,

electronic, spectroscopic, electromagnetic and chemical features of these finite systems with increasing size. With reducing particle size, the performance of surface atoms becomes dominant because at the lower end of the size limit. As can be seen from Figure 1, the surface atoms became dominant only when the palladium particle size reduced to below 10 nm.[15] Moreover, the properties changing with the particle size are also observed. For example, metal particles of 1–2 nm in diameter exhibit unexpected catalytic activity, as exemplified in catalysis by gold nanoparticles. While gold is chemical inert as bulk metal.[16]

1.2.2   Classification of Nanomaterials

From the forms of materials, nanomaterials are classified as zero-, one-, and two-dimensional nanostructures. 1) Zero-dimentional nanostructures, also named as nanoparticles, include single crystal, polycrystalline and amorphous particles with all possible morphologies, such as spheres, cubes and platelets. In general, the characteristic dimension of the particles is one hundred nanometres or bellow. Some other terminologies are zero-dimensional nanostructures: If the nanoparticles are single crystalline, they are often referred to as nanocrystals. When the characteristic dimension of the nanoparticles is sufficiently small and quantum effects are observed, quantum dots are the common term used to describe such nanoparticles. 2) One-dimensional (1D) nanostructures have been called by a variety of names including: whiskers, fibres or fibrils, nanowires and nanorods. In many cases, nanotubules and nanocables are also considered one-dimensional structures. Although whiskers and nanorods are in general considered to have smaller length to thickness ratio (aspect ratio) than fibres and nanowires, the definition is a little arbitrary. Therefore, nanostructures with large aspect ratio are addressed as "nanofibres" for clarity in this thesis, may they have been termed whisker, rod, fibre, wire before. 3) Thin films are two-dimensional nanostructures, another important nanostructure, and have been a subject of intensive study for almost a century, and many methods have

been developed and improved.

1.2.3   Synthesis Approaches and Techniques

In order to explore novel physical properties and phenomena and realise potential applications of nanostructures and nanomaterials, the ability to fabricate and process nanomaterials and nanostructures is the first corner stone in nanotechnology.

There are two approaches (Figure 2) to the synthesis of nanomaterials and the fabrication of nanostructures: top-down and bottom-up.[17] Top-down approach refers to slicing or successive cutting of a bulk material to get nanosized particles. Bottom-up approach refers to the build-up of a material from the bottom: atom-by-atom, molecule-by-molecule, or cluster-by-cluster. For example, milling is a typical top-down method in making nanoparticles, whereas the colloidal dispersion is a good example of bottom-up approach in the synthesis of nanoparticles. Both approaches play very important roles in nanotechnology.
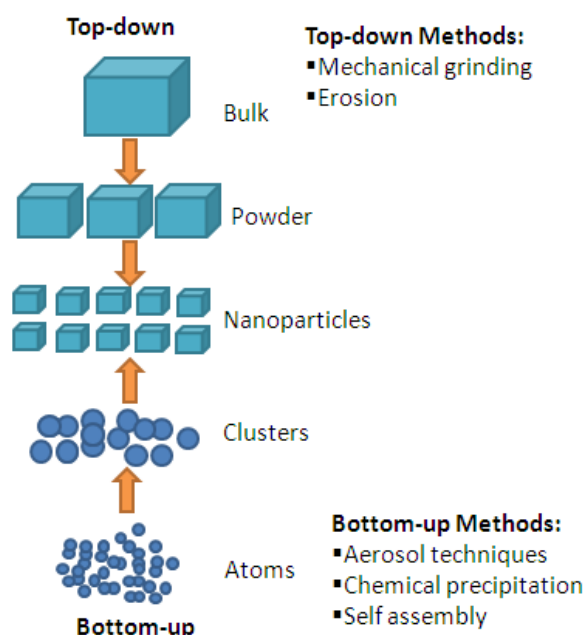
Figure 2. Schematic representation of the 'bottom-up' and 'top-down' approaches of nanomaterials. Adapted from ref 17.

These technical approaches can also be grouped according to the growth media:

(1) Vapour phase growth, including laser reaction pyrolysis for nanoparticle synthesis and atomic layer deposition (ALD) for thin film deposition.

(2) Liquid phase growth, including hydrothermal, colloidal processing for the formation of nanoparticles and self assembly of monolayers.

(3) Solid phase formation, including phase segregation to make metallic particles in glass matrix and two-photon induced polymerization for the fabrication of three-dimensional photonic crystals.

(4) Hybrid growth, including vapour-liquid-solid (VLS) growth of nanofibres.

The controlled growth of nanomaterials with different morphologies is of great importance because the difference in resulted exposed crystalline surface. Specifically, in catalytic applications, this controlling is necessary for improving selectivity. Zaera et al.[18] reported the tuning of selectivity, by controlling Pt particle shape, in the formation of cis olefins to minimize the production of unhealthy trans fats during the partial hydrogenation of edible oils.   The results shows clearly those tetrahedral Pt nanoparticles, which expose Pt (111) facets exclusively, exhibited better activity than sphere Pt particles with less (111) facets.

1.2.4   Characterisation Techniques

Characterisation of nanomaterials and nanostructures has been largely based on the surface analysis techniques and conventional characterisation methods developed for bulk materials. For example, X-ray diffraction (XRD) has been widely used for the determination of crystallinity, crystal structures and lattice constants of nanoparticles, nanofibres and thin films; scanning electron microscopy (SEM) and transmission electron microscopy (TEM) together with electron diffraction have been routine techniques used in characterisation of nanoparticles; optical spectroscopy is frequently used to determine the size of semiconductor quantum dots or the band gap and electronic structures of semiconductors.

Besides the established techniques of electron microscopy, diffraction methods and spectroscopic tools, scanning probe microscopy (SPM) is a relatively new characterisation technique and has found wide spread applications in nanotechnology. The two major members of the SPM family are scanning tunnelling microscopy (STM) and atomic force microscopy (AFM). Although both STM and AFM are true surface image techniques that can produce topographic images of a surface with atomic resolution in all three dimensions, combining with appropriately designed attachments, the STM and AFM have found a much broadened range of applications, such as nanoindentation, nanolithography, and patterned self-assembly. Almost all solid surfaces, whether hard or soft, electrically conductive or isolative, can all be studied with STM and AFM. Surfaces can be studied in gas (e.g. in air), in vacuum or in liquid.

1.3 Synthesis and Characterisation of Metal Oxide Nanostructures

From both fundamental and industrial standpoints, the development of systematic methods for the synthesis of metal oxide nanostructures is a challenge, as the first requirement in any study related to oxide nanostructures is the synthesis and characterisation of the material. Methods frequently used for the synthesis of bulk oxides may not work when aiming at the preparation of oxide nanostructures or nanomterials. For example, a reduction in particle size by mechanically grinding a reaction mixture can only achieve a limiting level of grain diameter, at best about 0.1μm. However, chemical methods can be used to effectively reduce particle size into the nanometre range. One of the most widely used methods for the synthesis of bulk metal oxide ceramics involves heating the components together at a high temperature over an extended period of time. However, elevated temperatures (>800 °C) can be a problem when using this approach for the generation of oxide nanostructures. A much better control of the product nanostructures can be achieved by direct co-precipitation (CP) of the oxide components from a liquid solution with

subsequent calcination, or by using sol-gels or microemulsions in the synthesis process. With these approaches, one can control the stoichiometry of the oxide nanostructures in a precise way. Such techniques are widely used for the synthesis of catalysts and ceramics. Chemical vapour deposition (CVD) is a technique employed in various industrial applications and technologies (e.g. the fabrication of sensors and electronic devices) that can be very helpful in the synthesis of oxide nanostructures.[19, 20] During the last decade, pulsed laser deposition (PLD) has been established as a versatile technique for the generation of nanoparticles and thin films of oxides.[21, 22] It is generally easier to obtain the desired stoichiometry for multi-element materials using pulsed laser deposition than with other deposition techniques.

Here we emphasise the description of 1D metal oxide nanostructures by hydrothermal method owing to the advantages in preparation of pure, well-dispersed, and well-crystallised products with controllable morphology. Specifically, the control of anisotropic growth is advanced by the use of directed templates, or by control of supersaturation, or by addition of capping agent.

1.3.1 Hydrothermal Method

Hydrothermal technique has been widely studied and employed in inorganic synthesis for many years. The term *hydrothermal* usually refers to any heterogeneous reaction in the presence of aqueous solvents or mineralisers under high pressure and temperature conditions to dissolve and recrystallise materials that are relatively insoluble under ordinary conditions.[23] The development of the hydrothermal technique was promoted by a gradually understanding of the mineral formation in nature under elevated pressure and temperature conditions in the presence of water. The studies dealing with laboratory simulations have helped the earth scientists to determine complex geological processes of the formation of rocks, minerals, and ore deposits.

The importance of the hydrothermal technique for the synthesis of inorganic compounds in a commercial way was realised after the successful synthesis of some products such as the use of sodium hydroxide to leach bauxite [invented in 1892 by Karl Josef Bayer (1871–1908) as a process for obtaining pure aluminium hydroxide which can be converted to pure Al_2O_3 suitable for processing to metal], and synthesis of large single crystal quartz (changed the tide of World War II) by Nacken and zeolite by Barrer (opened a new field of science - molecular sieve technology).[24-26]

Today, the hydrothermal technique has found its place in several branches of science and technology because of reduced contamination and low synthesis temperature, and this has led to the appearance of several related techniques with strong roots attached to the hydrothermal technique. The technique is being popularly used for crystallisation of materials, crystal growth, materials processing, thin film preparation, and so on. The detailed hydrothermal techniques and their advantages compared to other techniques for powder preparation are listed below:

- Powders are formed directly from solution
- Powders are anhydrous, crystalline or amorphous. It depends on producing of hydrothermal powder temperature
- It is able to control particle size by hydrothermal temperature
- It is able to control particle shape by starting materials
- It is able to control chemical composition, stoichiometry, and is ideal for metastable structure synthesis
- Powders are highly reactive in sintering
- Many cases, powders do not need calcination
- Many cases, powders do not need milling process

In recent years, with the increasing awareness of both environmental safety and the need for optimal energy utilization, there is a case for the development of

nonhazardous materials. These materials should not only be compatible with human life but also with other living forms or species. Also, processing methods such as fabrication, manipulation, treatment, reuse, and recycling of waste materials should be environmentally friendly. In this respect, the hydrothermal technique occupies a unique place in modern science and technology.
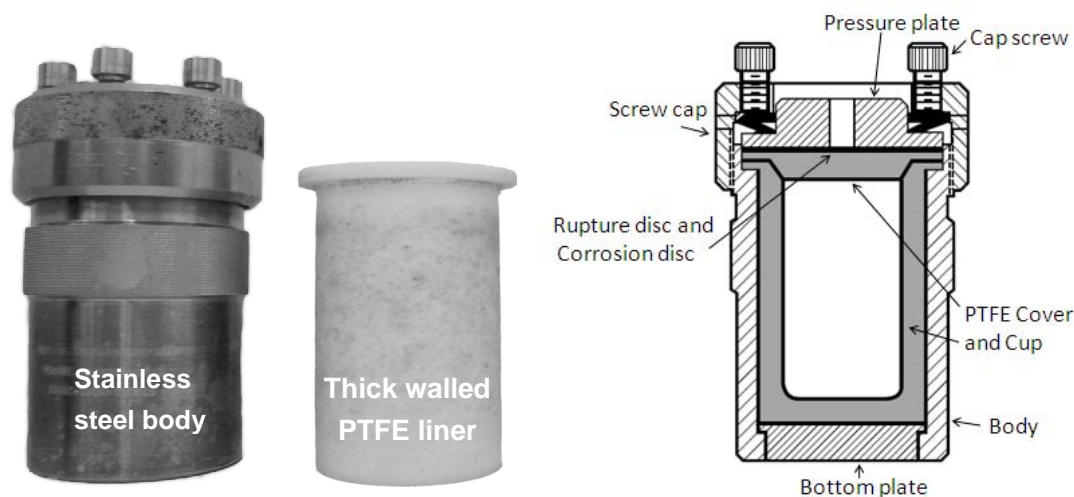
Figure 3. Photograph and schematic diagram of a typical laboratory autoclave from Parr (Acid digestion bomb, 125ml, Model 4748).

For a typical hydrothermal reaction, apparatus, called either "autoclaves" or "bombs", are used. A great deal of early experimental work was done using the Morey bomb (Morey 1953) and Tuttle-Roy test tube bomb (Tem-Press).[27] There are three types of companies providing commercial bombs in the US. (1) Tem-Press: They are the best source for research vessels of all kinds including test tube bombs and gas intensifiers for specialised gases, H_2, O_2, NH_3, etc. (2) Autoclave Engineers: They make a complete line of lab-scale valves, tubing, collars, all fittings for connections, etc and they also make very large autoclaves (1-3 m) for quartz and other chemical processes and (3) Parr Instrument: They make simple, low-pressure, low-temperature (300°C, 1000 bars) laboratory scale type of autoclaves, 50 mL - 1 L for low temperature reactions, including vessels lined Teflon (Figure 3; scheme of a typical bomb), etc. In addition to the conventional hydrothermal apparatus, microwave hydrothermal

apparatus have been applied for the synthesis developed by Komarneni and his cowokers.[28, 29] The application of microwave radiation during the process enhances the reaction kinetics by 1-2 orders of magnitude compared to the conventional hydrothermal processing. Milestone Company (Italy) provides advanced microwave hydrothermal instruments to accelerate sample preparation requirements within laboratory scale. However, the conventional apparatus are still widely used due to the easy-operation and low-cost behaviour.

Hydrothermal method has been widely used in the synthesis of metal oxide nanostructures for the unique advantages in the synthesis. Alkaline hydrothermal method has achieved a great success in the synthesis of 1D metal oxides nanostructures. In 1998, Kasuga et al. first reported a simple method for the preparation of TiO_2 nanotubes, without the use of sacrificial templates, by treatment of amorphous TiO_2 with a concentrated solution of NaOH (10 $moldm^{-3}$) in a polytetrafluoroethylene-lined batch reactor at elevated temperatures.[30, 31] In a typical process, several grams of TiO_2 raw material can be converted to nanotubes, with close to 100% efficiency, at temperatures in the range 110–150 °C, followed by washing with water and 0.1 mol/dm^{-3} HCl. It has since been demonstrated that all polymorphs of TiO_2 (anatase, rutile, brookite, or amorphous forms) can be transformed to the nanotubular or nanofibrous TiO_2 under alkaline hydrothermal conditions. The titanate fibres (typically $K_2Ti_6O_{13}$) was usually synthesised by pyrochemical process (conventional solid state reaction or a flux method). Berry et al. reported that potassium hexatitanate fibres could be obtained from the K_2O-TiO_2 system in supercritical water or molten KCl and from K_2O-TiO_2-KF melt systems in molten KCl.[32] Apparently, the particle size and morphology of the products are difficult to control and the resulted titanate is inevitable to exhibit low surface area. On the other hand, alkali titanate was also synthesised by a hydrothermal dehydration method from the $TiO_2 \cdot nH_2O$-KOH-H_2O system[33] for hexatitanate or from TiO_2 solid (or titanium complex such as $TiOSO_4 \cdot xH_2O$) and concentrated NaOH solution for trititanate[34].

14

Compared to pyrochemical method, hydrothermal method is of great advantage for the mild synthesis condition and vulnerable parameters. One can adjust the synthesis temperature, time, pressure (by external pressure or degree of filling of the autoclave), caustic soda concentration, solid-liquid ratio and additives to control the properties of product titanate. Thus, hydrothermal synthesis is promising because this method has many operation parameters to control particle size and morphology. A typical proof of the morphology control is the synthesis of titanate nanotubes. In fact, titanate nanotube is a metastable phase during the synthesis of titanate nanofibres by the reaction between TiO_2 and concentrated NaOH solution. In a typical synthesis the optimum synthesis temperature for titanate nanotubes and nanofibres is 150 and 180 °C, respectively, when using rutile powder and 10 M of NaOH solution as reactants.[34] While by adjusting the synthesis procedure, a direct hydrothermal hydrolysis from anatase TiO_2 to large quantities of pure multiwall crystal titanate nanotubes (with almost uniform inner diameters of 5 nm, outer diameters of 10 nm and lengths of about 300 nm), was realised at 100 - 180 °C in 5 - 10 M NaOH solution.[35] In addition, the hydrothermal method has also been applied for preparing other metal oxide nanostructures. $NaNbO_3$ with cube morphology and $K_4Nb_6O_{17}$ particles were synthesised by employing nearly the same procedure for the preparation of titanate nanofibres. [36-39]

Binary metal oxides such as VO_x nanotubes,[40] MnO_2[41] and MoO_3[42] nanofibres are also obtained through a hydrothermal process. VO_x nanotubes are easily accessible in high yield by hydrothermal treating a precursor, which is prepared by treating a vanadium(v) oxide with an amine ($C_nH_{2n+1}NH_2$ with $4 \leq n \leq 22$) or an α,ω-diaminoalkane ($H_2N[CH_2]_nNH_2$ with $14 \leq n \leq 20$), and following hydrolyzation, and aging of the gel.[40] The lengths of the VO_x nanotubes vary in the range 0.5 ± 15 μm and the outer diameters in the range 15 ± 150 nm. Hydrothermal method has also been developed in the synthesis of a MnO_2 (both α and β phase) nanofibers by Li et al.[41] through the oxidation of Mn^{2+} by $S_2O_8^{2-}$, α-MnO_2 nanofibres morphology with

diameters 5-20 nm and lengths ranging between 5 and 10 μm, while β-MnO$_2$ samples show nanorod morphology with diameters 40-100 nm and lengths ranging between 2.5 and 4.0 μm. The direct transformation of MoO$_3$·2H$_2$O into MoO$_3$ nanorods was achieved by Paktze et al.[42] through a hydrothermal process: autoclave treatment of the starting material with small amounts of a solvent, preferably an acid, results in the quantitative formation of fibrous MoO$_3$. In a standard procedure, MoO$_3$·2H$_2$O is simply treated with diluted glacial acetic acid in an autoclave (180 °C, 7 days). Plain nanorods with an average diameter of 100 ± 150 nm and lengths on the microscale (3 ± 8 μm) are formed quantitatively. After washing off the acid and drying in air, the product is pure.

Hydrothermal reactions have been widely applied for the synthesis of 1D metal oxide nanostructures. From a mechanistic point of view, the fact for the hydrothermal synthesis that the solid is first dissolved completely and then precipitates again clearly excludes any kind of topotactic reaction. Consequently, the anisotropic morphologies may be generated in this straightforward step, which can be deliberately controlled to prepare intermediate products. Therefore, a thorough investigation is necessary to generalise the underlying reaction principle and so to exploit it for the synthesis of other nanomaterials.

1.3.2   Post-treatment/Modification

To obtain a nanomaterial is not the end of the synthesis process. Based on the understanding of the structure, there is a lot can be done toward modifying the structures thus adjusting the physical and chemical properties.

Alkali titanates are series of compounds with the formula A$_2$Ti$_n$O$_{2n+1}$ (A = Li, K, Na), which normally show unique layered (3 < n < 5) and tunnel (6 ≤ n ≤ 8) crystal structures (two typical structures, Na$_2$Ti$_3$O$_7$ and Na$_2$Ti$_6$O$_{13}$, are shown in Figure 4).

Titanates are also well known functional ceramic materials (dielectric, piezoelectric, ferroelectric etc.) and titanate-fibres are widely used as structural reinforcements in polymers, metals and ceramic-composites because of their outstanding mechanical properties and thermal stability.[43] Owing to the layered structure, the alkali metal ions are exchangeable with H^+ ions, other metal ions or organic cations. From alkaline hydrothermal method, layered titanate phase was directly obtained. A post-treatment process is needed to achieve TiO_2 phase.[44] There are two comprehensive reviews already exists in this intensely researched field by Chen et al.[45] and Bavykin et al.[12] summarised recent findings on titania and titanate (nanofibres and nanotubes) based materials.
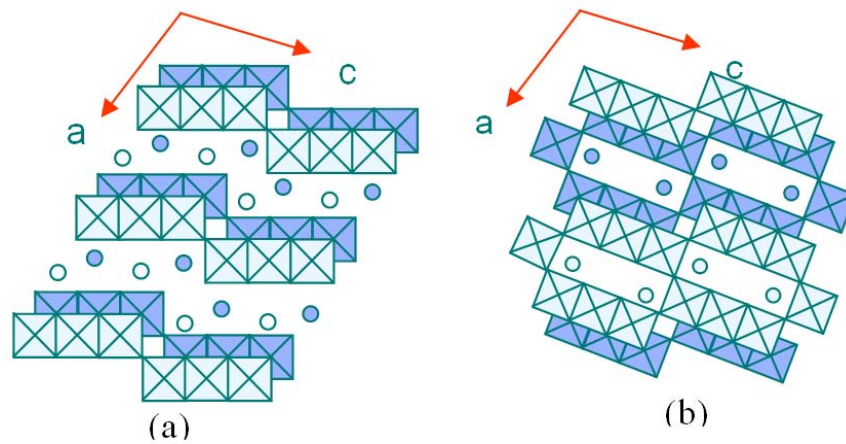
Figure 4. Schematic illustration of the layered structure $Na_2Ti_3O_7$ (a) and the tunnel structure $Na_2Ti_6O_{13}$ (b). Both views are along the *b*-axes. Adapted from ref 44.

The synthesis of titanate via hydrothermal method is also of great advantage for achieving various functional structures through subsequent phase transformation, because the products from hydrothermal process are active for reaction. The phase transformation is a very interesting and complicated process. Taking the phase transformation of $Na_2Ti_3O_7$ as an example, one can obtained single crystal fibres of $TiO_2(B)$ and anatase by post-treatment of the alkali titanates prepared from a hydrothermal process (Figure 5). The resulted titanate of hydrothermal reaction is Na-titanate ($Na_2Ti_3O_7$) when concentrated NaOH solution and TiO_2 power were

employed for the synthesis. The Na cations can be exchanged with H^+ ions after washing with dilute HCl acid, yielding H-titanate ($H_2Ti_3O_7$).[12, 43] By calcination of H-titanate at designated temperatures, one can obtain three phase of TiO_2 fibres ($TiO_2(B)$, anatase and rutile). In addition to the conventional calcination method, acid assisted phase transformation method was also employed for the transformation from H-titanate to TiO_2 phase (anatase and rutile). More interestingly, the reaction between titanate and titania of different phases is reversible - the as-obtained titania can react with concentrated NaOH to form trititanate. The $Na_2Ti_3O_7$ can also be transformed to a thermal stable phase $Na_2Ti_6O_{13}$ by calcination at 500 °C in air.[44] In the applications of TiO_2 as photocatalyst, the phase transformation knowledge is useful for modification of the photocatalyst structure to improve its activity.
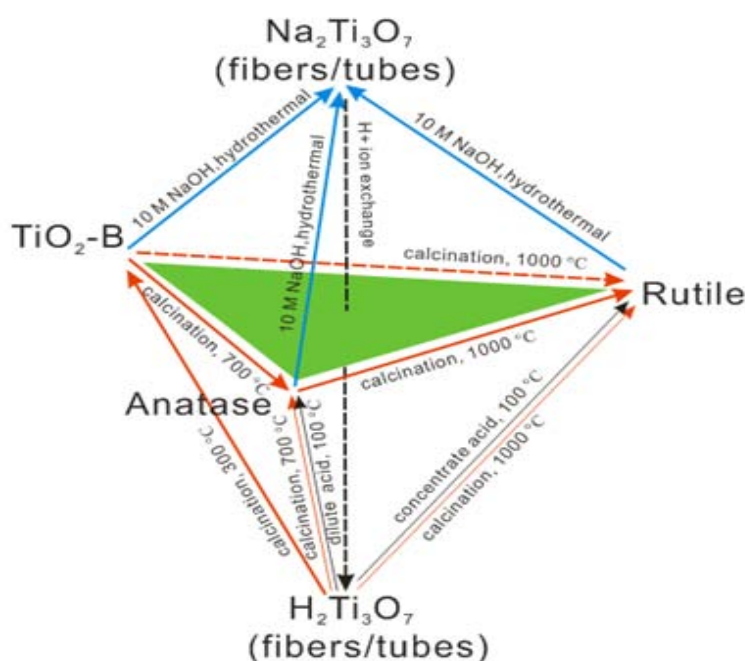
Figure 5. Diagram of the phase transformation between titanate and TiO_2 phases.

Metal cations can be incorporated into the layer structure of titanates due to the ion exchange ability. Li et al. conducted a number of experiments to introduce transit metal ions, such as Cd^{2+}, Zn^{2+}, Co^{2+}, Ni^{2+}, Cu^{2+}, and Ag^+, into the structure of titanate nanotubes in an aqueous ammonia solution.[35] Products were carefully washed with dilute ammonia and deionised water several times to avoid physical adsorption of the

18

substituting ions on the surface of the titanate nanotubes. The transition-metal ions substituted titanate nanotubes show the modified magnetic and optical properties. Moreover, transparent thin films of the propylammonium/Ti_3O_7 intercalation compound was fabricated through exfoliation and restacking of the powders of layered titanate $Na_2Ti_3O_7$ by propylammonium ions.[46] The transparent thin film of the propylamonium/Ti_3O_7 intercalation compound is valuable as a host for functional molecules such as dyes due to its expandable two-dimensional nanospace and macroscopic anisotropy.

1.3.3   Surface Structure Characterisation
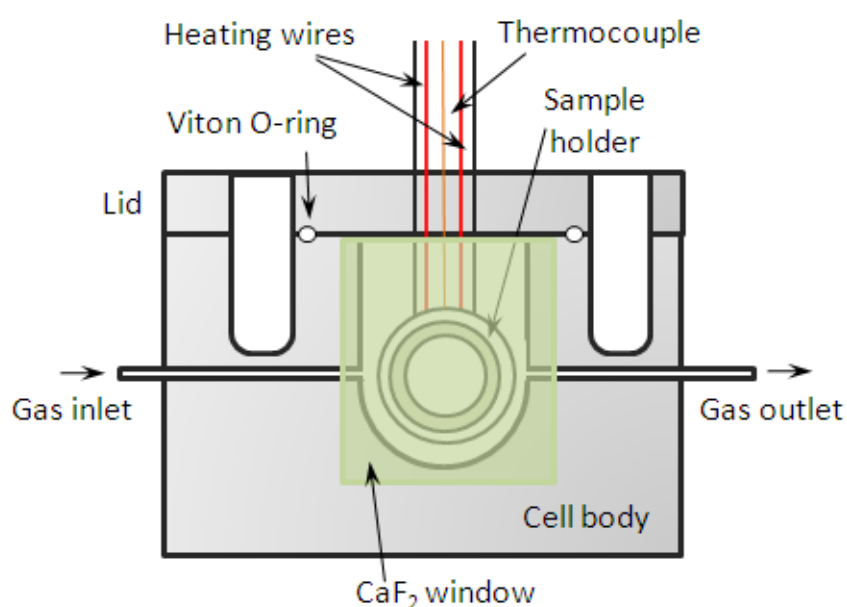
Figure 6. Sample cell employed for simultaneous gas adsorption and IR spectral measurements. Adapted from ref 51.

The surface of nanomaterials plays an import role for the small size effect as stated in Section 1.2.1. Moreover, metal oxides are largely served as catalysts,which permit reaction takes place on the surface.[47, 48] It is necessary to study the surface properties, such as surface structure and species adsorbed on the surface. To do such a study in a systematic way, one needs a diverse array of experimental techniques (X-ray

diffraction and scattering, microscopies, vibrational and electron spectroscopies, etc.). Besides these commonly used characterisation techniques for the nanomaterials, the surface analysis techniques can provide useful information as the surface sites play a more important part in nanostructures properties. Temperature programmed desorption (TPD) is an effective method to study the surface adsorbed groups for understanding of the mechanism of catalysis and photocatalysis.[49] Also, IR spectroscopy with a special sample cell (with IR window, see Figure 6) which permitts evacuation, gas inlet, and heating of the sample is advance for the study of the surface absorbents.[50, 51] The cell can act as a microreactor, which is stated to operate over a temperature range from 300 to 870 K and up to 5 bar total pressure. If such a reactor is connected to the usual reactant and product gas lines, the catalyst performance can be monitored by gas chromatography (GC) or mass spectrometry (MS) analysis.
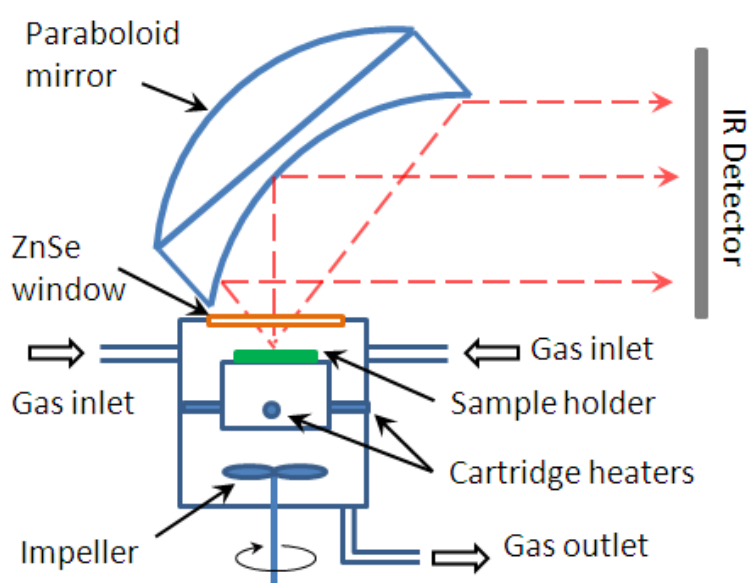
Figure 7. Schematic description of in situ infrared emission cell (Adapted from Ref 52).

IR emission technique is also a useful tool to study the catalyst surface adsorbed species. According to Kirchoff's law, the infrared emission spectrum of a heated

sample contains the same information as the absorption spectrum. Figure 7 shows the schematic design of an infrared emission cell for in situ catalyst studies reported by Sullivan et al.[52] The infrared emissivity is proportional to the fourth power of the temperature difference between the emitting sample and the detector, and at medium to high temperatures (below 1000 K) black-body emission shows a maximum in the mid-infrared region of the spectrum. The disadvantage is that the resolution depends on the difference between the sample and the detector and it is difficult to obtain good spectra at low temperature. The advantage of the IR emission technique lies on that it is possible to monitor both structural changes in the catalyst and adsorbed species at the same time. While in transmission spectra of oxide or zeolite disks, the characteristic metal-oxygen stretching modes and zeolite lattice bands are normally too intense to be observed. In emission spectra,

The use of tools such as scanning tunnelling microscopy (STM) and other imaging techniques has greatly enhanced the understanding of the structure of thermally-created defects on the $TiO_2(110)$ surface. Much work has been done by a number of different groups with STM to better understand the nature of surface defects. Moreover, theoretical methods (ab initio and semi-empirical quantum-mechanical calculations, Monte Carlo simulations, molecular dynamics, etc.) are also important to help understanding the structure.[53]

1.4 Applications of Metal Oxide Nanomaterials

Within the last decade, many areas of the industry have witnessed the advent of nanoscience. This section is focused on the technological uses of nanostructured oxides as catalysts, photocatalysts. Other applications involving absorbents, and ceramic materials, are also summarised here.

1.4.1   Catalysts

Metal oxides have wide industrial applications in catalysis field by serving as active compositions or as supports. There are a lot of opportunities in modifying nanostructures to improve substantially the catalytic activity and selectivity of existing catalysts. Such endeavours are particularly fruitful when a fundamental approach is adopted, whereby the design of the catalyst composition and microstructure is targeted towards solving the bottleneck of specific reactions.

Basic Concepts. Catalysts are species that are capable of directing and accelerating thermodynamically feasible reactions while remaining unaltered at the end of the reaction. They cannot change the thermodynamic equilibrium of reactions.[5, 54] The performance of a catalyst is largely measured in terms of its effects on the reaction kinetics. The catalytic activity is a way of indicating the effect the catalyst has on the reaction rate and can be expressed in terms of the rate of the catalytic reaction, the relative rate of a chemical reaction (i.e. in comparison to the rate of the uncatalysed reaction) or via another parameter, such as the temperature required to achieve a certain conversion after a particular time period under specified conditions. For example, the term turnover frequency (TOF) in catalysis is used to describe molecules reacting per active site in unit time. Catalysts may also be evaluated in terms of their effect on the selectivity of reaction, specifically on their ability to give one particular reaction product. In some cases, catalysts may be used primarily to give high reaction selectivity rather than high conversion rate. Stability is another important catalyst property since catalysts are expected to lose activity and selectivity with prolonged use. This then opens the way to regenerability which is a measure of the catalyst's ability to have its activity and/or selectivity restored through some regeneration process. Catalytic processes are the application of catalysts in chemical reactions. In chemicals manufacture, catalysis is used to make an enormous range of products: heavy chemicals, commodity chemicals and fine chemicals. Catalytic

processes are used throughout fuels processing, in petroleum refining, in synthesis gas ($CO + H_2$) conversion, and in coal conversion. More recently, the demand for clean technology or environment protection has driven most of the new developments in catalysis.

Catalysis is described as homogeneous when the catalyst is soluble in the reaction medium and heterogeneous when the catalyst exists in a phase distinctly different from the reaction phase of the reaction medium.[55] Almost all homogeneous catalytic processes are liquid phase and operate at moderate temperatures (<150 $^{\circ}$C) and pressures (<20 atm). Corrosion of reaction vessels by catalyst solutions, and difficult and expensive separation processes are common problems. Traditionally, the most commonly employed homogeneous catalysts are inexpensive mineral acids, notably H_2SO_4, and bases such as KOH in aqueous solution. The chemistry and the associated technology is well established and to a large extent well understood. Many other acidic catalysts such as $AlCl_3$ and BF_3 are widely used in commodity and fine chemicals manufacture via classical organic reactions such as esterifications, rearrangements, alkylations, acylations, hydrations, dehydrations and condensations. More recently, there have been significant scientific and technological innovations through the use of heterogeneous catalysis, involving a solid catalyst that is brought into contact with a gaseous phase or liquid phase reactant medium in which the catalyst is insoluble. This has led to the expression "contact catalysis" sometimes used as an alternative designation for heterogeneous catalysis.

Metal Oxide Supported Au catalysts. It is noted that the metal oxide supported noble metal nanoparticles is a class of very important catalysts. Numerous investigations using supported gold catalysts on metal oxides were carried out during last two decades since the pioneer work by Haruta et al.[56, 57] Before this, gold was regarded as catalytic inactive. It becomes an incredible active material when subdivided into nanoscale. Catalysis by supported gold catalysts has rapidly become a

hot topic in chemistry, and has found widely applications in reactions such as selective oxidation of alcohols, oxidation of CO, reduction of selective reduction of nitro groups. Good reviews on gold catalysis are available by Huntings et al. and Arcadi. [58, 59]

It is generally agreed that the catalytic activity of gold catalysts depends on the size of the gold particles since the Au catalyst is totally inactive when the particle size is larger than ~8 nm in diameter.[60, 61] Developing practical methods for the preparation of supported-Au catalysts with good control of Au particle size and stability still remains a challenge.[56, 60] Various methods such as deposition-precipitation (DP),[62-65] co-precipitation (CP),[65-68] and impregnation (IP)[69-72] have been developed to prepare controllable gold particles uniformly supported on substrates.
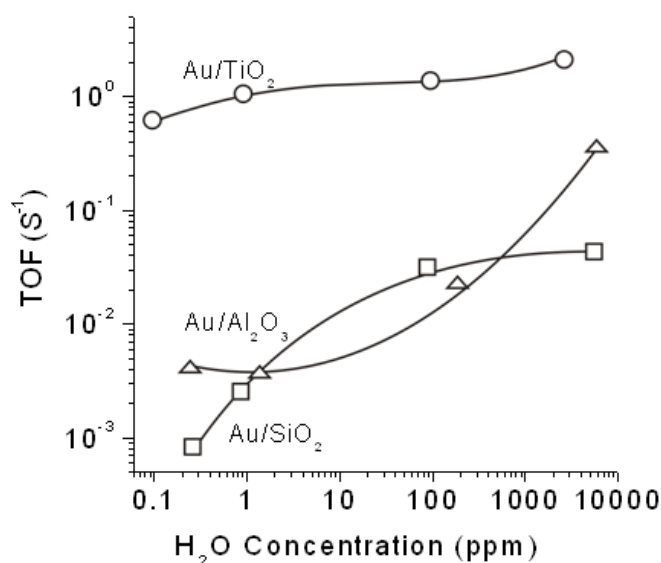
Figure 8. Turnover frequencies (TOF) per surface gold atom at 273 K for CO oxidation over a) Au/TiO_2, b) Au/Al_2O_3 and c) Au/SiO_2 as a function of moisture concentration. Adapted from Ref 77.

A support with large specific surface area allows well dispersion of Au particles on the support surface. Nanofibres and nanotubes are suitable to serve as supports because of their large surface area. Zhu et al.[73, 74] loaded gold particle on TiO_2

(anatase) nanotubes and nanofibres using deposition-precipitation (DP) method, in which small gold particles and high catalytic activity for CO oxidation are obtained as a result. Moreover, the nature of oxides is also of great importance as the activities are related to it. Metal oxides, such as ZrO_2, Al_2O_3, TiO_2 and SiO_2 are widely used catalyst supports. Oxides supported gold catalysts are active towards many reactions, including oxidation of CO, selective oxidation (alkenes, alcohols and even alkanes), water-gas shift, and removal of atmosphere pollutants (NO_x, VOCs). The supports used are classified as reproducible and irreproducible supports. The gold samples loaded on reproducible samples show high activity toward CO oxidation.

An interesting found on supported gold catalysts is that moisture plays an essential role in low-temperature CO oxidation, by contributing to the formation and regeneration of the surface active sites.[75, 76] Haruta et al. reported that this effect of the moisture is dependent on the catalyst support.[75, 77] As is shown in Figure 8, the enhancement of activity with the increasing moisture concentration was observed on the different types of supports involving insulating Al_2O_3 and SiO_2 as well as semiconducting TiO_2. However, so far a detailed mechanism involving the role of moisture and that of catalyst supports have not been well addressed. In a recent coupled TG-FTIR study on Au/α-Fe_2O_3 catalysts for CO oxidation,[78] it was proven that at low temperatures, small Au nanoparticles cannot activate the oxygen of the support lattice directly, and thus the lattice oxygen doesn't participate in the reaction; instead, it is molecular oxygen species that are responsible for the low temperature CO oxidation. Meanwhile, there are a lot of reports showing that the activation of molecular O_2 occurs mainly on the catalyst support,[75, 79, 80] and are probably related to the surface OH groups and to the surface O-vacancy concentration and distribution. On the other hand, the extensive studies on the photocatalytic water splitting reaction on TiO_2 surface,[81] have shown that water molecules can either dissociate at oxygen vacancies (defects) on the TiO_2 surface, yielding surface OH groups, or physically adsorb on these sites. Theoretical studies have revealed that surface OH-groups on

TiO$_2$ can facilitate adsorption and activation of molecular oxygen.[82, 83] Based on the above knowledge, a logical hypothesis could be proposed, in which the defect sites on TiO$_2$ surface may play a key role in the catalytic oxidations using molecular O$_2$ as oxidant. The enhanced O$_2$ and H$_2$O adsorption due to these defects results in increased activity. Therefore, a systematic study of the surface structure and the activity are necessary to explain this phenomenon.

1.4.2 Photocatalysts
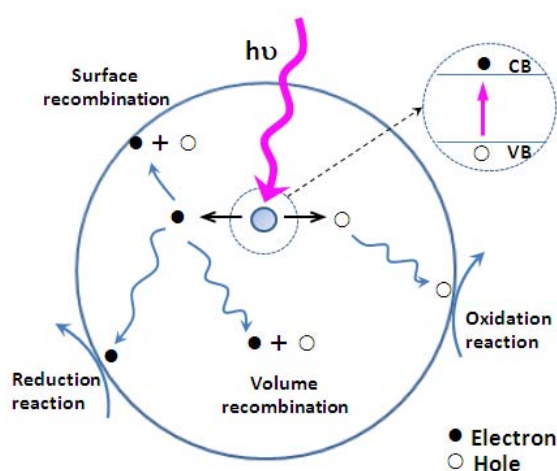
Figure 9. Schematic illustration of the charge separation theory of semiconductor upon a photoexcitation. Adapted from ref 49.

The energy that the Earth receives from the Sun is gigantic: 3×10^{24} joules a year, which is about 10,000 times more than the global population currently consumes.[84] In other words, if we could only exploit 0.01% of this incoming solar energy for the profit of humankind, we could solve the problem of energy shortage. Any improvement in the utilization of sunrays will make a profound positive effect on modern science and technology. In 1972, Fujishima and Honda discovered the photocatalytic splitting of water on TiO$_2$ e1ectrodes, which is the first photocatalyst suitable for water splitting   and the beginning of a new era of modern heterogeneous photocatalysis.[85] Thereafter, a great deal of effort has been devoted to photoeletrochemical process such as splitting of water,[86, 87] reduction of carbon

dioxide for the conversion of solar energy into chemical energy[88, 89] and wet-type solar cells.[84] In addition to applying photocatalysts for energy renewal and energy storage, applications of photocatalysts to environmental cleanup have been one of the most active areas in heterogeneous photocatalysis.[90-92] This is inspired by the potential application of TiO_2 based catalysts for the complete destruction of organic contaminants in polluted air and waste water.[49, 53, 93]

The power of semiconductor based photocatalyst, such as TiO_2, is due to charge separation ability (Figure 9). When a semiconductor is illuminated under a light with energy larger than the band gap, there will be an excitation of an electron from the valence band to the conduction band, leaving a hole at the valence band.[49] The separated hole has strong oxidation power to obtain electron from absorbed species. The separated charge and hole can also recombine to release energy in heat form. To enhance the photocatalysis, electron-hole pair recombination must be suppressed. This can be achieved by trapping either the photogenerated electrons or the photogenerated holes at trapping sites in the structure.
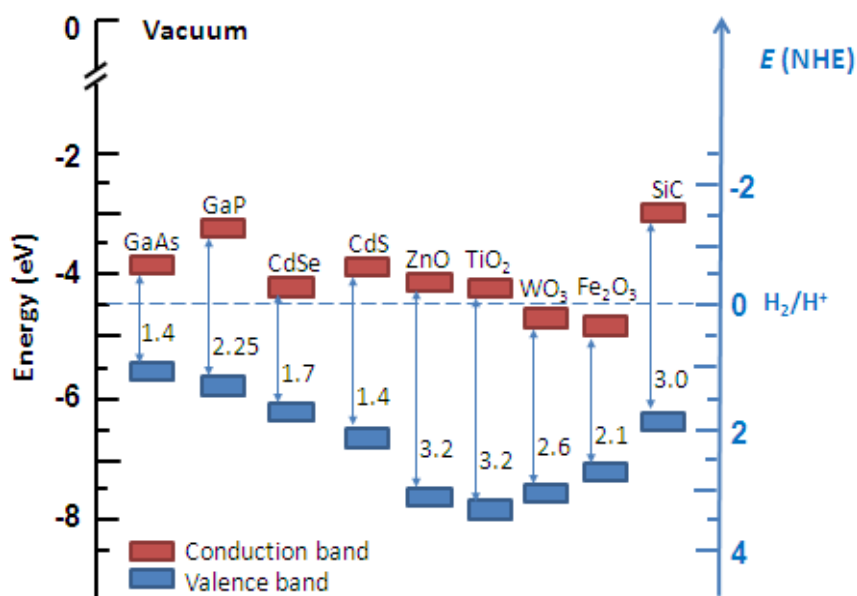
Figure 10. Energy diagrams for various semiconductors in aqueous electrolytes at pH = 1. Adapted from ref 84.

The band gap of a semiconductor determines its working wavelength. The semiconductors with either too large or too narrow band gaps are not suitable for practical use. The reason is that larger band gap will not cause any reaction while narrow band gap materials will have to face the problem of light erosion. The band gaps of different semiconductors are shown in Figure 10. Till now, TiO_2 (anatase, bandgap ~3.2 eV) is the most extensively studied material for photocatalysts because of its strong oxidizing power, low toxicity, and long-term photostability.[49, 92, 94] TiO_2 exists mainly in four polymorphs in nature, anatase (tetragonal, space group $I4_1/amd$), rutile (tetragonal, space group $P4_2/mnm$), brookite (orthorhombic, space group Pbca) and TiO_2(B) (monoclinic, space group C2/m).[95, 96] TiO_2(B) is a metastable monoclinic polymorph of titanium dioxide, which can be synthesised from titanate,[12, 97-100] sol-gel method[101] and is also found in nature.[102] The rutile phase is the most thermal stable phase at the macroscale.[103] Anatase phase is considered to have higher photoactivity than other phases.[104-106] The band gap of TiO_2(B) and rutile are in a range of 3-3.22 eV,[107, 108] slightly narrower than that of anatase (3.2-3.3 eV).

To improve the photocatalytic efficiency, various of modification methods including transition metal doping (V, Cr, Fe), nonmetal doping (N, S, C), noble metal loading and building mixed phase interface have undertaken to improve the overall photocatalytic activity of TiO_2. There are already good reviews exist in ***Chem. Rev.*** by Yates et al. in the modifications of TiO_2 photocatalysts.[49, 53] While most of the present studies are based on the modification of anatase crystals, the modification based on titanates and subsequent transformation to TiO_2 may provide more advanced structures with a better activity.

An advantage of the modification of titanate 1D nanostructures is that the modifications can be conducted in early stages, from the synthesis of layered titanate nanofibres or nanotubes instead of on anatase nanofibres. Metal doped titanate

nanofibres were achieved by addition of metal in the hydrothermal synthesis process. As mentioned in Section 1.3.2, layered structure possesses an important ion-exchangeable ability. Metal ions can be doped through a simple ion-exchange step (increasing of the treating temperature is needed at some case to increase the diffusion rate of dopant ions).

1.4.3 Other Applications

Metal Oxides as Absorbents. Environmental contaminations caused by radioactive ions from the tailings and heap-leach residues of uranium mining industry (such as ^{226}Ra ions), the by-product of nuclear fission reaction (such as ^{90}Sr) and the leakage of the nuclear reactor may cause long-term problems that sometimes are serious threat to the health of a large population. To address the serious problem, techniques must be developed for removal of the radioactive ions from environment (mainly from waste water) and safe disposal of them. The core issue of such technology is to devise materials that are able to absorb these ions irreversibly, selectively, efficiently and in large quantities from contaminated water. Besides, the sorbent materials should be very stable to radiation, chemicals, thermal and mechanical changes so that the ions can be safely disposed together with the sorbent. Currently, available absorbents such as activated alumina, zeolite, activated carbon, and silica gel cannot fulfil the task for safe disposal. New and better absorbents are required to meet the challenges. Nanostructured layered metal oxides are expected to play a prominent role as effective absorbents for the above-mentioned applications. They possess high surface areas and have a large surface-to-bulk ratio compared with conventional oxides; a great deal of fundamental and applied research is yet to be carried out in this very promising and interesting area.

Oxide Nanomaterials in Ceramics. The traditional ceramics, normally silicate-based ceramics, usually associated with art, dinnerware, pottery, tiles, brick, and toilets.

Despite these traditional products have been, and continue to be, important to society, a new class of ceramics is emerging. These advanced or technical ceramics are being used for applications simply unexpected (or even unknown) some years ago, such as chemical processing and environmental ceramics, engine components, computers and other electronic components, or cutting tools.[4] Advanced ceramics are distinguished from traditional ceramics by their larger strength, higher operating temperatures, improved toughness, and tailorable properties. Chemical processing and environmental ceramics include filters, membranes, catalysts, and catalyst supports.

Ceramic separation membranes are of particular interest in many separation processes because they can be used under severe conditions with a long operation life, owing to their chemical and thermal stability.[20, 109-111] They are able to function unaffected within organic and biological systems and at high temperatures, can be readily cleaned (or sterilised) by using steam treatment, and exhibit long operational lives. The low energy consumption and absence of potentially harmful chemical agents in the separation processes using ceramic membranes, for both gases and liquids, also presents additional economic and social impetus.[20, 109] These outstanding and compelling features have resulted in the rapid adoption of ceramic membranes within the dairy, food, pharmaceutical, bioengineering, chemical, nuclear-energy, water treatment, and electronic industries.[20, 109-114]

1.5 Aims of the Thesis

Article 1: Structural Evolution in a Hydrothermal Reaction between Nb_2O_5 and NaOH Solution: From Nb_2O_5 Grains to Microporous $Na_2Nb_2O_6 \cdot 2/3H_2O$ Fibres and $NaNbO_3$ Cubes

1. To investigate the reaction activity in the hydrothermal reaction between Nb_2O_5 and concentrated NaOH solution.

2. To symmetrically study the influence of the hydrothermal parameters (e.g. temperature, time, concentration) on the structural properties of the final product, and achieve controllable synthesis.

3. To synthesise the possible existing metastable structures of niobium oxides utilizing the knowledge obtained in hydrothermal reaction.

4. To discover the general reaction mechanism between metal oxides and concentrated NaOH solution by monitoring the product at different stages.

5. To determine the structure obtained with varying characterisation techniques.

Article 2: Contribution of the Interface of Mixed Anatase and $TiO_2(B)$ Phases Nanofibres to the Photocatalytic Activity and Determination of the Interface Structure

1. To obtain more delicate titanate nanosturctures by hydrothermal synthesis method and post-treatment process.

2. To achieve mixed-phase nanostructures consisted of anatase and $TiO_2(B)$ and investigate their photocatalytic performance.

3. To determine the interface structure of the mixed anatase and $TiO_2(B)$ phase nanofibres using TEM and EDP techniques.

4. To verify the charge separation theory, widely accepted in P25 system, in the systems of mixed TiO_2 phases as long as there is a sufficient difference between the conduction band edges, irreversible charge transfer from one

phase will occur and can enhance the photocatalytic activity of the mixed-phase TiO_2 catalysts.

Article 3: Correlation of the Catalytic Activity for Oxidation Taking Place on Various TiO_2 Surfaces with Surface OH-Groups and Surface Oxygen Vacancies

1. To synthesis and investigate TiO_2 nanomaterials with different chemical surface sites.

2. To load gold on nanostructured TiO_2 surface to produce new catalysts for photocatalysis and thermal catalysis, and study the catalytic activities.

3. To study the reactivity of the products in different reactions, identify the common features between them, and correlate the activity and surface structure to find out the structural factors that influence the catalytic reactions.

Article 4-5: Titanate Nanofibres as Intelligent Absorbents for the Removal of Radioactive Ions from Water

1. To synthesis different titanate nanostructures with large cations exchange ability and study the adsorption properties.

2. To determine the adsorption uptake capacity of radioactive ions (Ra, Sr) and examine the structure change caused by the adsorption (Article 4).

3. To investigate the performance of titanate nanofibres for the adsorption of heavy metal ions from water (Article 5).

4. To investigate the competition adsorption (selectivity) in the presence of rich Na ions.

5. To investigate the release of the adsorbed ions to determine whether the absorbent is suitable for permanent disposal.

Article 6-7: High-Performance Ceramic Membranes with a Separation Layer of Metal Oxide Nanofibres

1. To develop new ceramic separation membranes with high efficiency by using the metal oxide nanofibres as building blocks

2. To optimise the membrane preparation to achieve hierarchical structures with superior separation property and mechanical strength.

3. To investigate the performance (selectivity, flux) of the constructed membrane.

1.6 Note from the Author

This thesis is compiled as seven consecutive published journal articles. Four of these papers are collaborated work and listed in Chapter 5 as supporting information. Preceding each chapter is short introductory remarks from the author. These include discussion of specific motivations for our research direction that will help the reader immediately grasp the content of the article. For example, the introductory may include the theoretical approaches before the experiment. Also, the important results we have obtained but not included in the journal papers will be mentioned. The main aim of these preceding sections is to justify the logical relationship of articles in

different chapters. Please note that a full bibliography is given as a separate chapter (Chapter 7) that covers all references for the content of the thesis (Literature Review, Introductory Remarks, and Conclusions) except the main particles.

CHAPTER 2. STRUCTURAL EVOLUTION IN A HYDROTHERMAL REACTION BETWEEN Nb_2O_5 AND NaOH SOLUTION: FROM Nb_2O_5 GRAINS TO MICROPOROUS $Na_2Nb_2O_6 \cdot 2/3H_2O$ FIBRES AND $NaNbO_3$ CUBES (ARTICLE 1)

2.1 Introductory Remarks

This article is the first report on the controlled synthesis of various niobate nanostructures using hydrothermal method. The main aim of this article is to present the role of kinetic reaction controlling to tune the composition, crystallite and morphology of nanostructure as well as the detailed structure characterisation of these nanostructures utilizing different techniques.

Using hydrothermal reaction for the synthesis of metal oxides has become a hot topic for the advantages it brings as stated in the first chapter, and tremendous research papers about this technique appear on journals. In this group, a detailed study on the synthesis of titanate structures via an alkaline hydrothermal process has been conducted in the past few years.[34, 43, 115] It shows that either nanofibres or nanotubes structure can be obtained by subtle control of the reaction conditions. These materials showed promising applications in photocatalysis, and Li-ion storage for battery. To apply our knowledge on the synthesis of other metal oxide systems is of great importance for the possibility of obtaining new nanostructures. On the other hand, alkali niobates have emerged as a novel material with enormous technological and scientific interest because of their excellent nonlinear optical, ferroelectric, piezoelectric, electricoptic, ionic conductivity, pyroelectric, photorefractive, selective ion exchange, and photocatalytic properties.[116-120] The great potential of these

materials has stimulated research on their synthesis.[29, 36-39, 121-126] Alkaline niobate powders are usually synthesised by a solid state reaction of heating alkaline and niobium pentoxide at temperatures of 800 °C or above.[19, 117-120, 127, 128] Sol-gel methods, using alkoxide precursors and complexes with organic compounds, were also reported for the synthesis.[121, 122, 124, 126] Kormarneni et al. found that niobium oxide powder reacted with an aqueous solution of potassium hydroxide at 194 °C yield crystalline $KNbO_3$.[29] An outstanding advantage of such a hydrothermal synthesis is that the reaction temperature required to produce niobate crystalline is much lower than those in other methods. Recently, potassium niobates ($K_4Nb_6O_{17}$ and $KNbO_3$)[37, 39] and sodium niobate ($NaNbO_3$)[36, 38] have been synthesised by the reaction of Nb_2O_5 solid with concentrated KOH or NaOH solution under hydrothermal reaction. While for niobium oxide hydrothermal synthesis, there is only reported that it can reacted with KOH and obtained a cubic structure under hydrothermal condition. Considering hydrothermal reaction is advanced for yielding the metastable structures, detailed work for the reaction between niobium oxide and NaOH should be performed to obtain the various nanostructures which may pose different functions.

In this study, the detailed the reaction behaviour of Nb_2O_5 under alkaline hydrothermal condition was studied. This involves: 1) Adjusting of the reaction temperature to investigate the reaction activity; 2) Controlling the reaction time to monitor the reaction stages. SEM was employed to monitor the morphological evolution of the niobate products in such a reaction, and it provides a clear and direct picture of the reaction process. These niobates were characterised by XRD, TEM/HRTEM, NMR, TGA, Raman, UV-vis and PL spectroscopies. Moreover, the attempt to investigate the ion exchange ability of these niobates has been conducted.

2.2 Article 1

CHAPTER 3. CONTRIBUTION OF THE INTERFACE OF MIXED ANATASE AND TiO$_2$(B) PHASES NANOFIBRES TO THE PHOTOCATALYTIC ACTIVITY AND DETERMINATION OF THE INTERFACE STRUCTURE
(ARTICLE 2)

3.1 Introductory Remarks

In recent years, TiO$_2$ has emerged as a promising photocatalyst for the removal of organic pollutants from waste water and polluted air and till now, TiO$_2$ is still the most important photocatalyst in practical applications. As stated in the first chapter, intense illumination has to be applied while using TiO$_2$ based photocatalysts, for the low quantum efficient resulting from high recombination rate. Therefore, methods to lower the recombination rate in the catalyst are of great significant to enhance the photocatalytic activity. It is reported that the high activity of TiO$_2$ P25, which is composed of mixed anatase and rutile phases, is attributed to the charge separation process induced by the existence of bang gap difference in the mixed-phase structure. TiO$_2$(B) has a similar band gap structure with rutile, if we can constructed the mixed phase of anatase and TiO$_2$(B), it is very likely that we can prepare another efficient photocatalyst. This is also a contribution to the theoretical study of the theory that mixed-phase structure can enhance the photocatalytic activity.

This chapter deals with the influence of the mixed-phase nanostructure of titania [anatase and TiO$_2$(B)] on the activity of photocatalytic decomposition of organic pollutants. We have successfully synthesised several titanate nanostructures. The as-obtained titanates, prepared from hydrothermal methods, are layered structure with

Na ions can be exchanged with proton. The protonated titanate can yield TiO_2 of anatase or $TiO_2(B)$ phases depends on the calcination temperature.[129, 130] Based on these knowledge, we develop a new nanostructure, anatase and $TiO_2(B)$ mixed-phase nanostructure with different molar ratio, by a facile calcination of titanate at controllable temperatures. The mixed-phase structure was compared with the most famous TiO_2 photocatalyst, P25. The activities of the mixed-phase structures and pure anatase $TiO_2(B)$ were compared. And the interface structure between these two phases was worked out with the help of HRTEM and EDP techniques.

Following this study, a new core-shell structure, which consisted of mixed-phase nanofibres with a shell of anatase nanocrystals on the fibril core of $TiO_2(B)$, was prepared by hydrothermal reaction and subsequent treatment. Anatase crystals coated on $TiO_2(B)$ cores has a preferred orientation to form well matched interfaces. These interfaces were proven to reduce charge recombination and thus enhance the photocatalytic activity. For details of the work, please refer to the fourth paper in the publication list.

3.2 Article 2

This article is not available here.
Please consult the hardcopy thesis
available from QUT Library

Supporting Information:

Structure and Contribution to Photocatalytic Activity of the Interfaces in Nanofibers with Mixed Anatase and TiO$_2$(B) Phases

Zhanfeng Zheng, Hongwei Liu, Jianping Ye, Xueping Gao, Jincai Zhao, Eric R. Waclawik, Huaiyong Zhu*

To estimate the fraction of TiO$_2$(B) phase in the mixed phase samples, a calibration curve was made experimentally using mixtures of TiO$_2$(B) and anatase with known phase compositions. The mixtures were prepared by mechanically mixing T500 [pure TiO$_2$(B) phase] and T700 (pure anatase phase) at designed mass ratios. XRD patterns of these mechanical mixtures with TiO$_2$(B) fractions of 98%, 95%, 90%, 80%, 70%, 60%, 50%, 40%, 30%, 20%, and 10% were given in Fig. S1. When the fraction of TiO$_2$(B) phase was below 10%, it became difficult to detect the diffraction of this phase in the mixture under the instrumental conditions of the present study. The plot of the intensity ratio of the diffraction peak at 33.4° for TiO$_2$(B) to that at 37.8° for anatase phase against the fraction of TiO$_2$(B) in the mixtures was used for constructing a calibration curve (Fig. S2). One can estimate the TiO$_2$(B) fraction in a sample containing the two phases from the calibration curve using the intensity ratio of the sample under investigation because an intensity ratio value corresponds to a fraction on the calibration curve.
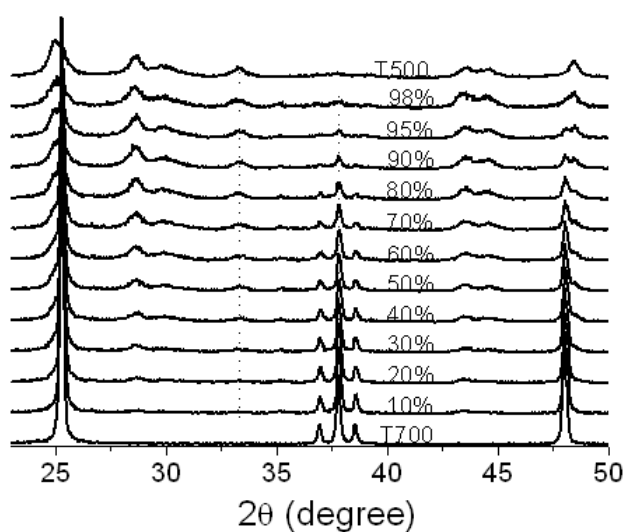
Fig. S1. XRD patterns of mechanical mixtures of TiO$_2$(B) and anatase, the anatase fractions in the mixtures are 90%, 80%, 70%, 60%, 50%, 40%, 30%, 20%, 10%, 5%, and 2%, respectively.
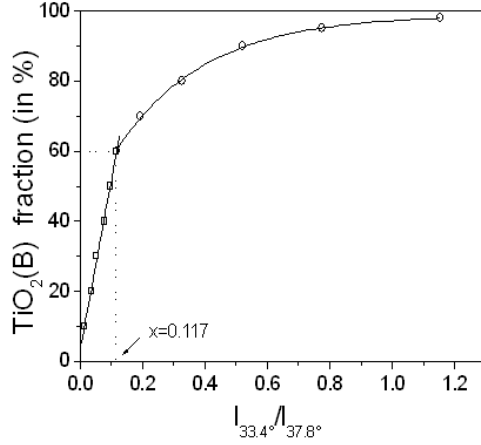
Fig. S2. The calibration curve for the relation between $TiO_2(B)$ fraction and the intensity ratio ($I_{33.4°}/I_{37.8°}$) of the peak at 33.4° to the peak at 37.8°, which correspond to ($\bar{3}11$) plane of $TiO_2(B)$ (JCPDS 74-1940) and (004) plane of anatase (JCPDS 21-1272), respectively.

When the intensity ratio ($I_{33.4°}/I_{37.8°}$) < 0.117, the calibration curve fits well with equation (1); when the ratio >0.117, it fits with equation (2).

$$y = 4.855x + 0.029 \qquad (1)$$

$$y = 0.988 - \frac{13.156}{1 + e^{(0.849+x)/0.276}} \qquad (2)$$

Besides, the average crystallite sizes of anatase and $TiO_2(B)$ were estimated from the line broadening of corresponding X-ray powder diffraction peaks (24.9° for $TiO_2(B)$ and 25.4° for anatase) according to the Scherrer equation. As shown in Table 1, the crystallite size increases gradually with increasing calcination temperature.
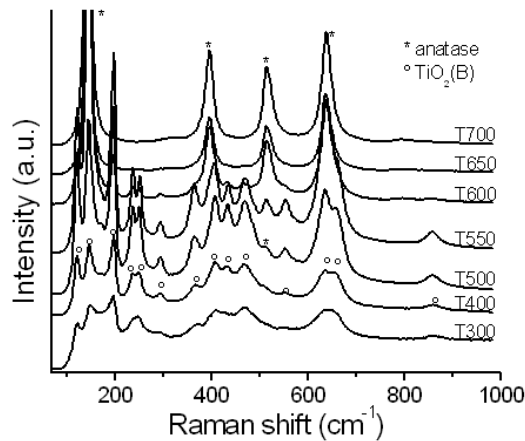
Fig. S3. Raman spectra of fibrous TiO_2 photocatalysts calcined at various temperatures with excitation line at 633 nm.

60
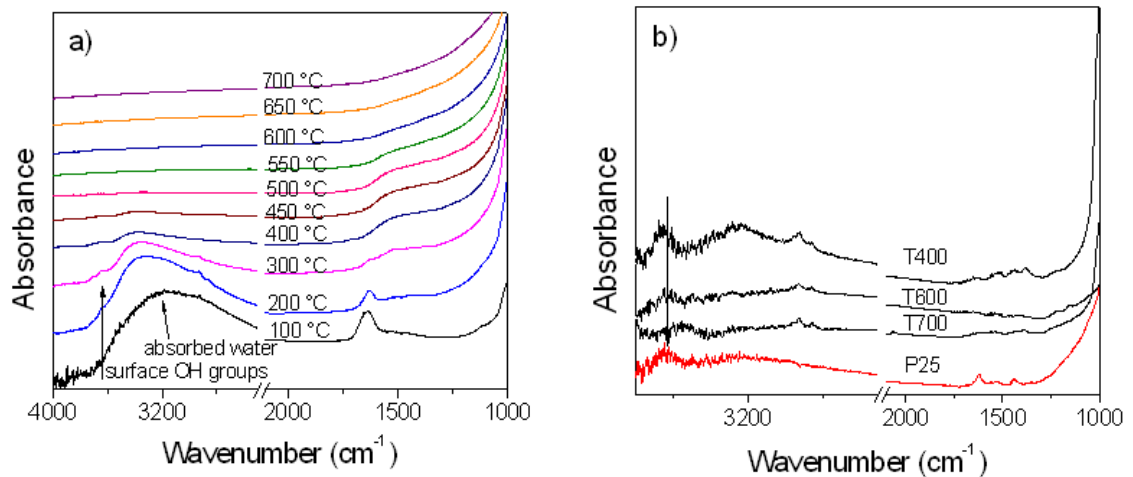
Fig. S4. IES spectra of a) H-titanate conducted from 100 to 700°C, and b) the typical samples showed rehydroxylation of after exposure to moisture (spectra are taken at 100 °C).
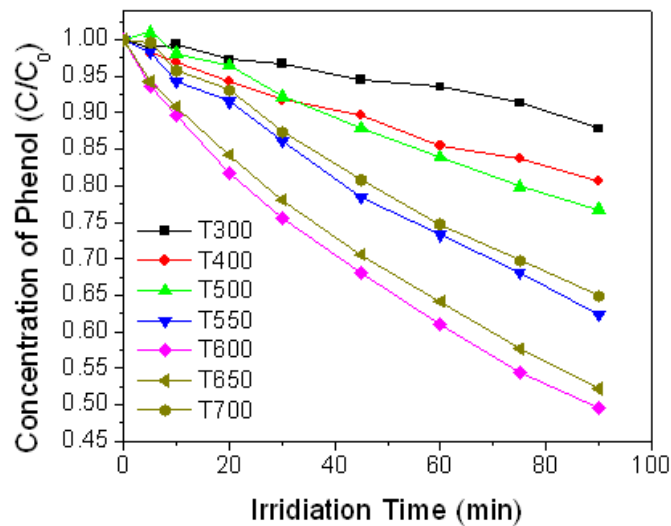
Fig. S5. Photocatalytic decomposition of phenol with different fibril TiO_2 photocatalysts under UV irradiation.
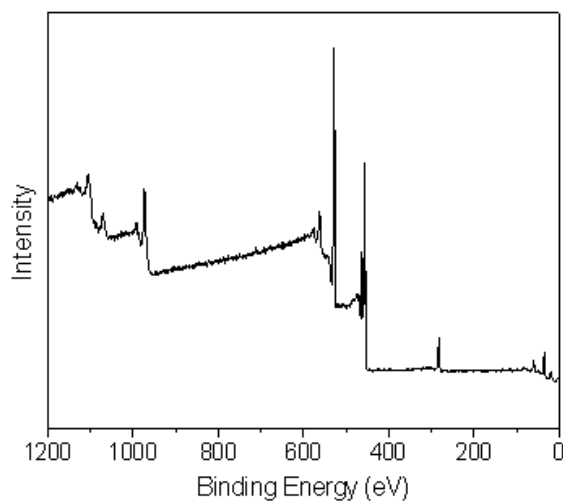
Fig. S6. XPS spectra of the H-titanate fibers.
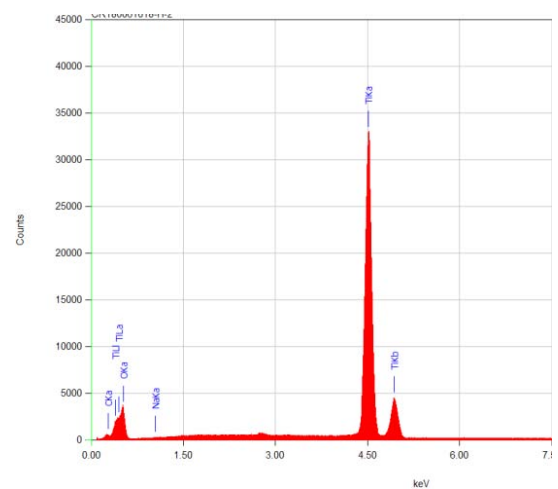
Fig. S7. EDS pattern of the starting H-titanate.

CHAPTER 4. CORRELATION OF THE CATALYTIC ACTIVITY FOR OXIDATION TAKING PLACE ON VARIOUS TiO$_2$ SURFACES WITH SURFACE OH-GROUPS AND SURFACE OXYGEN VACANCIES
(ARTICLE 3)

4.1 Introductory Remarks

This chapter deals with the role of surface structure on the activity of TiO$_2$ photocatalysts or their supported gold catalysts. As stated in the introductory of Chapter 2, we have successfully synthesised titanate nanofibres and nanotubes, which can convert to TiO$_2$(B) and anatase phases. We have developed a new structure with anatase and TiO$_2$(B) mixed-phase by simple calcination of titanate at various temperatures. In the preceding article, the detailed structure of mixed-phase nanofibres was studied. As the catalytic reactions take place on the surface,[47] therefore, it is also necessary to study the surface structure of the material for a better understanding of the mystery behind it. With the technique for the synthesis of TiO$_2$ nanostructures of various phases, we constructed TiO$_2$ nanostructures with different surface structures. Here, three reactions were studied to understand the influence of different surface structures.

The first is using Au/TiO$_2$ as photocatalysts for the removal of Volatile organic compounds (VOCs) driven by visible light. This is based on the surface plasmon resonance (SPR) effect of gold nanoparticles while absorbing visible light intensely (Figure 11). The electromagnetic field of incident light couples with the oscillations of conduction electrons in gold particles, resulting in strong-field enhancement of the local electromagnetic fields near the rough surface of gold nanoparticles.[131] The

enhanced local field strength can be over 500 times larger than the applied field for structures with sharp apices, edges, or concave curvature (e.g. nanowires, cubes, triangular plates, and nanoparticle junctions). The SPR absorption may cause rapid heating of the nanoparticles. This is proved by a series of experiment conducted in our lab by studying the activity for the oxidizing of VOCs on gold particles loaded on different large band gap metal oxides such as ZrO_2 and SiO_2. The bare oxides do not show activity because of the large band gap. This work is designed to work out the original activity of TiO_2 supported gold particles compared with large band gap oxides supported gold particles.
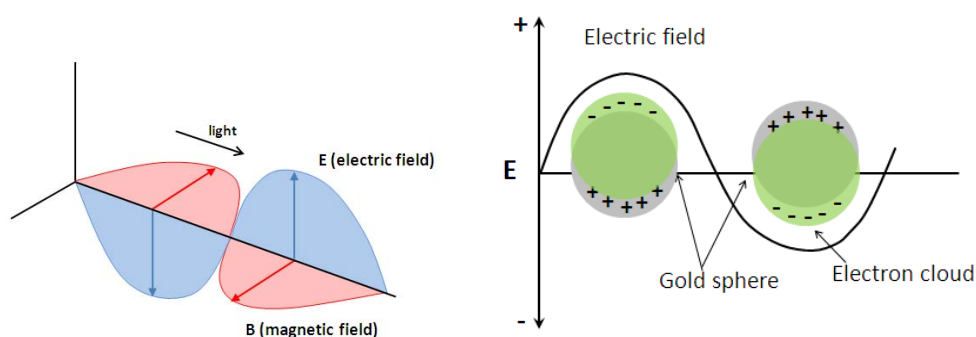
Figure 11. Schematic illustration of SPR effect - the delocalised electrons in the metal clusters can undergo a collective excitation, which has large oscillator strength, typically occurs in the visible part of the spectrum and dominates the absorption spectrum. The electromagnetic radiation (e.g. light), as the name implies, contains both an electric and a magnetic component (the left diagram). Adapted from ref 131.

The second reaction is the oxidation of CO at room temperature on these supported gold catalysts and the third is the photocatalytic oxidization of SRB in aqueous solution under UV light irradiation with TiO_2 nanosturctures (without gold). In all these reactions, there is a common feature that molecular oxygen was used as oxidant. Considering the same chemical composition of these structures, the activity difference should come from the difference in the surface structures.

Therefore, in this paper, FT-IR emission spectroscopy (IES), a technique allowing us to investigate the surface change of solids during heating, was employed for the study

of the surface structures. This technique has long been used to characterise the surface OH groups on metal oxides. It was reported recently that OH groups can facilitate the O_2 adsorption. Correlating the OH properties on oxides surface and the role of OH groups in catalytic and photocatalytic reactions, we can explain the dependence of the activities on surface structure.

4.2 Article 3

This article is not available here.
Please consult the hardcopy thesis
available from QUT Library

Supporting Information:

Figure S1. Raman spectra of acid treated H-titanate (evidence that an anatase thin layer formed).
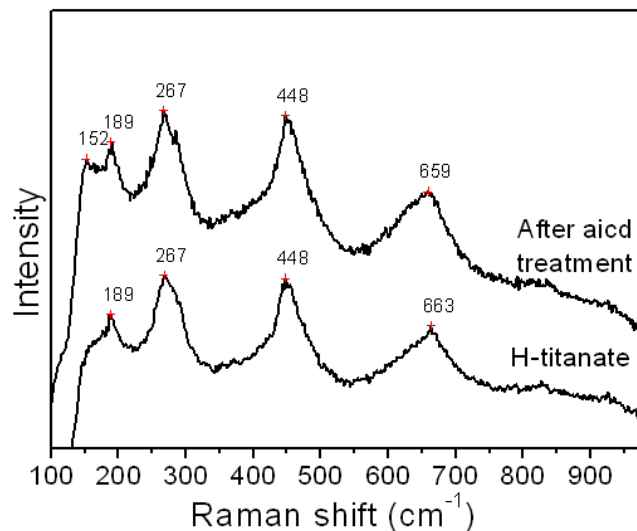
Figure S2. Surface structures of exposure planes in anatase; (a) HRTEM of anatase nanorod; (b) plane (001); (c) plane (101), note that the normal of the plan (101) is [601]. The array of bridging oxygen ions are shown as light yellow and possible oxygen vacancy is marked by black-color arrows.
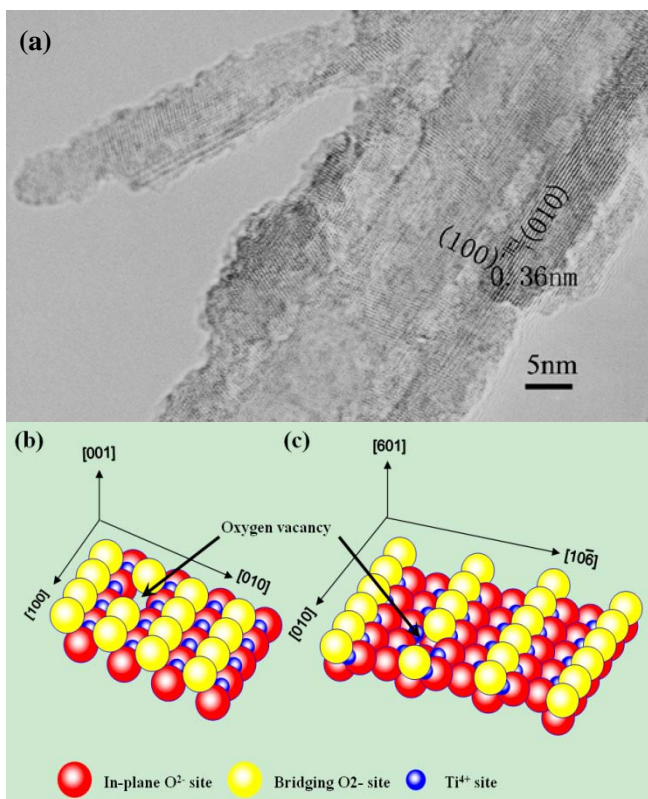
CHAPTER 5. SUPPORTING INFORMATION (ARTICLE 4 - 7)

5.1 Introductory Remarks

Because of the unique properties of titanate nanofibres, both from the structure and morphology, they have many applications. This chapter illustrates the development of applications of titanates in other areas, in addition to the applications in photocatalytic and catalytic fields.

As Absorbents. Titanates have been considered as a possible nuclear waste host for decades.[132, 133] These materials are usually fabricated by pyrochemical process in commercial scale and available for various uses. The titanate nanofibres can be prepared readily by hydrothermal reactions between caustic soda and a titanium compounds (even industrial grade rutile minerals) and the manufacturing cost is relatively low. The ion-exchange ability of the layered titanate allows them to adsorb radioactive and heavy metal ions as observed in our experiment. The fibril sorbents can be readily dispersed into a solution because the fibres do not aggregate seriously as clay and zeolites. Moreover, the absorbents can be readily separated from a liquid after the sorption by filtration, sedimentation, or centrifugation because of their fibril morphology. Also, the titanate structure can convert to other forms with different layered (e.g. $Na_2Ti_3O_7$) or tunnel (e.g. $Na_2Ti_6O_{13}$) structures. The attribution may show the potential selectivity adsorption of the some cations in a special size range. The exchange of bivalent radioactive cations may also result in the structural collapse thus trapping the cations in the solids permanently for safe disposal. Therefore, this study is of great significance for the environment remediation. A detailed study on the adsorption properties of tunnel structured $Na_2Ti_6O_{13}$ has also been conducted, yet not

shown here.

As Ceramic Membrane Materials. The porous ceramic separation membranes have an unsymmetrical layered structure, consisting of a macroporous (pore size >400 nm) support, a porous intermediate layer, and a nanoporous top layer.[20, 109-114] The support and layers are usually fabricated from oxide particles because the voids between the particles can form passageways through the membrane (i.e. continuous porosity), which can be used for filtration. The thick macroporous support (of up to several millimetres) provides the necessary mechanical strength of the membrane. The intermediate layer is usually applied to the macroporous support next to prevent the small particles used to form the top layer from blocking the pores in the support. Such blocking can substantially reduce the flux through the membrane.[109] The top layer is usually applied to the intermediate-layer macroporous support using sols of metal hydrates.[20, 109-114] The sols are applied layer by layer in order of decreasing size of sol particles to achieve interparticle voids that are effective for separation. The selectivity of the membrane is controlled solely by the pore size of the top layer, and the flux passing through the filter depends, predominantly, on the thickness of the top layer. Therefore, the top layer fulfils the actual separation function of the membrane. However, the top layers of the ceramic membranes fabricated using conventional approaches are aggregates of particles, and are unable to permit a high flux while maintaining good selectivity.[112, 113, 134-141] In addition, the conventional approach encounters significant difficulties because of the formation of pinholes and cracks during the drying and calcination process, and a dramatic loss of flux when pore sizes are reduced to increase selectivity.

To achieve ceramic membranes with high efficiency, we have to introduce radical changes in the membrane texture: the membrane texture is crucial to the separation efficiency and should be of primary concern when developing separation membranes. In the traditional sieves for separation of the bulk particles, they are made of wires to

increase the efficiency of mesh structure. The aggregates of metal oxide fibres exhibit more large porosity than particles with other shape, therefore, if we can coat a large porosity substrate uniformly with the nanofibres in a thin layer, they should form a ceramic top layer that permits high selectivity while maintain high activity.

5.2 Article 4

This article is not available here.
Please consult the hardcopy thesis
available from QUT Library

5.3 Article 5

This article is not available here.
Please consult the hardcopy thesis
available from QUT Library

5.4 Article 6

This article is not available here.
Please consult the hardcopy thesis
available from QUT Library

5.5 Article 7

This article is not available here.
Please consult the hardcopy thesis
available from QUT Library

CHAPTER 6. CONCLUSIONS

The main conclusions of the thesis as a result of research project are listed below. More detailed explanation is presented in the following discussion.

1. **Hydrothermal synthesis of niobate nanostructures.** The structure evolution of niobates in the hydrothermal reaction between Nb_2O_5 and concentrated NaOH was monitored and it was found that we could control the reaction kinetics to obtain the desired nanostructures. The hydrothermal technique has shown its advantages in the synthesis of metastable nanostructures.

2. **Mixed-phase anatase/TiO_2(B) nanostructure.** Mixed-phase TiO_2 photocatalyst exhibited better photocatalytic activity than either the pure anatase or TiO_2(B) phase. This is due to the suppression of the recombination process by separation of electron-hole pair through the irreversible interphase charge transfer.

3. **The role of surface OH groups on metal oxides.** The ability of various TiO_2 nanostructures to generate surface OH groups was identified by IES technique. As the OH groups can facilitate the O_2 (oxidant in reaction) adsorption and activation during the catalytic or photocatalytic reaction, the TiO_2 nanostructures with stronger ability to regenerate surface OH groups can exhibit better activity. In addition, a new mechanism for the Au/TiO_2 activity toward photodecomposion of VOCs is proposed.

4. **Layered titanate absorbents.** Titanates with different layered structures, including a new metastable titanate, were successfully synthesised. These titanates proved to be effective absorbents for the removal of radioactive cations by trapping these cations and forming stable structure.

5. **Titanate nanofibres for the construction of nanofibers.** A new generation of ceramic membrane was successfully constructed by applying titanate nanofibres and boehmite nanofibres as top layer. They exhibit high selectivity while

maintaining high flux compared to the traditional membrane made of particles.

One of the advantages of the metal oxide nanostructures studied in this thesis is that they can be produced economically in large quantities by a one-pot alkaline hydrothermal process at a relatively mild condition. Moreover, the facile controlling of phase transformations of the metal oxides with retained fibril structure provides more opportunities for further functionalising the materials. The fibril metal oxides show wide applications in catalysis, photocatalysis, adsorption and ceramic separation membrane. Therefore, intended synthesis of metal oxides material and further modification of the nanostructures based on the understanding of the detailed structure and the properties they possess, as well as the reactions will allow us to obtain new functional materials with broad applications.

In Chapter 2, we demonstrate a first report of sodium niobate nanofibres prepared from alkaline hydrothermal method. The morphological evolution of the solid in the reaction between Nb_2O_5 and concentrated NaOH solution was monitored by SEM. In the reaction between NaOH solution and Nb_2O_5, the corner-sharing of NbO_7 decahedra and NbO_6 octahedra is ruptured first. Next, in NaOH solution, the microporous fibres with monoclinic lattice, $Na_2Nb_6O_{13} \cdot 2/3H_2O$, crystallise and grow at the expense of the poorly crystallised niobate consisting of NbO_6 octahedra that are linked by edge-sharing. The delicate microporous molecular sieve structures of the fibres are confirmed by XRD, HRTEM, ^{23}Na MAS NMR techniques, and Li^+ ion exchange experiment are consistent with those reported in the literature. By carefully optimizing the temperature and length of the reaction, one can achieve high-purity fibres with a delicate structure by direct reaction between concentrated NaOH solution and Nb_2O_5 powder. The optimal combination of the reaction temperature and time is at 180 °C for 120 min. The important feature of the synthesis of the present study is that selection of the fibril product is achieved by control of reaction kinetics. The final product for the continuing reaction at 180 °C is $NaNbO_3$ cubes. Such a structural conversion results in a remarkable change in light absorption. Therefore, this study is of importance for developing new function materials by wet chemistry process.

In Chapter 3, this study addresses two important general issues regarding mixed-phase photocatalysts. First, it demonstrates the theory that the difference between band edges of two phases in intimate contact can facilitate charge transfer from one phase to another, and thus reduce the recombination of photogenerated electrons and holes. This is applicable to the photocatalysts of mixed $TiO_2(B)$ and anatase phases. The interfaces between the two phases have a function of lowering charge recombination and enhancing the activity for photocatalytic oxidation of SRB. Second, the atomic arrangement of the interfaces between the two phases was determined for the first time. We found that the two phases closely match each other at the interface at an atomic level, and this structure facilitates the charge transfer. This could be general feature for stable interfaces between two phases in mixed-phase catalysts. Thus the above information is useful for understanding the mechanism of the photocatalytic reactions on the mixed-phase catalysts. The determination of interface structure of metal oxides is an important frontier in solid-state inorganic chemistry. The progress in this aspect is of general significance and may be extended to other metal oxide systems. In addition, a series of mixed-phase nanofibres were prepared by relatively simple process, and they are efficient photocatalysts in terms of activity, mechanical strength and separation after uses.

In Chapter 4, we prepared four types of TiO_2 nanotubes and nanorods, and loaded 3wt% of gold to these TiO_2 solids by sonication treatment of $HAuCl_4$ solution employing lysine as the capping agent and $NaBH_4$ as reduction reagent. Au/TiO_2 catalysts were used for the photocatalytic oxidation of HCHO in air at 20°C under blue light (with wave length between 400 and 500 nm) and for CO oxidation at moderate temperatures in gas phase. In all the cases, various TiO_2 phases supported Au catalyst showed the same activity sequence with the rehydroxylation ability of the bare TiO_2 supports. Correlating the surface OH groups regeneration ability and the activity, we tentatively proposed the oxidation mechanism: the oxygen vacancies at bridging O^{2-} sites of titania surface can generate surface OH-groups that facilitate adsorption and activation of O_2 molecules and enhance catalytic activities of titania solids and gold catalysts supported the titania solids for catalytic and photocatalytic oxidations with molecular O_2 as oxidant; and the ability to generate surface OH-groups is an indicator of the catalytic activity.

In Chapter 5, titanate nanofibres prepared by hydrothermal method with formulas, $Na_2Ti_3O_7$, $Na_{1.5}H_{0.5}Ti_3O_7$, were used to remove the bivalent radioactive and heavy metal ions from wastewater, such as $^{90}Sr^{2+}$, $^{226}Ra^{2+}$, and Pb^{2+} ions. They exhibit larger sorption capacities of these toxic ions than the traditional absorbents, such as layered clays and zeolites. The sorption by the titanate fibres is also much faster than those by the traditional absorbents. The fibres can selectively adsorb M^{2+} ions in the presence of Na^+ ions whose concentrations are much larger than that of the target M^{2+} ions. More importantly, the sorption can cause considerable deformation of the layered structure in nanofibres when approaches a certain extent. Most of the adsorbed toxic M^{2+} ions were trapped permanently in the nanofibres because of the structure deformation and could not be released from the fibres to water. So the toxic cations can be safely deposed after sorption without further treatment.

We constructed ceramic nanoporous filters with a hierarchically structured separation layer on a porous substrate using larger titanate and smaller boehmite (AlOOH) nanofibres. The randomly oriented titanate nanofibres can completely cover the rough surface of the porous substrate of micrometre α-alumina particles, leaving no pinholes or cracks. On top of this titanate fibre layer, a layer of γ-alumina fibres was formed using boehmite nanofibres. The resulting membranes can effectively filter out species larger than 60 nm at flow rates orders of magnitude greater than with conventional membranes, and they do not have the structural deficiencies of conventional ceramic membranes. The use of ceramic nanofibres or nanorods, instead of particulates with irregular shapes, to fabricate ceramic membranes is a new direction in developing high-performance ceramic membranes. A mesh structure of threads should be the most efficient structure for filtration, achieving high selectivity and maintaining much higher flux than membranes of other forms. Conversely, nanofibres of various metal oxides and hydrous oxides, including copper oxide, alumina, silica, titanate, and rare-earth oxides have been synthesised recently. The dimensions of these nanofibres

cover a wide range. For instance, by adjusting the synthesis conditions we can tailor the thickness of boehmite fibres from 3 to 10 nm, and the length from 40 to 100 nm, or tailor the thickness of titanate fibres from 10 nm to 100 nm and the length from 100 nm to 20–30 μm. These inorganic nanofibres can be readily dispersed in aqueous or alcohol solutions. This allows us to construct layers of randomly oriented fibres (LROF) on a porous ceramic substrate as the separation layer by applying thin layers of dispersed nanofibres. Furthermore, we can construct hierarchical LROF structures, in which layers of the smaller fibres lie on top of layers of larger fibres, so that the selectivity of the membranes can be controlled within a wide range. The resulting membranes with such a structure should possess the merits of ceramic membranes, being able to withstand steam cleaning and regeneration at high temperatures. These properties are crucial for practical application of the ceramic membranes.

CHAPTER 7. BIBLIOGRAPHY

1. J. L. G. Fierro, *Metal Oxides: Chemistry and Applications*, CRC Press, Florida, 2006.
2. V. E. Henrich, P. A. Cox, *The Surface Chemistry of Metal Oxides*, Cambridge University Press, Cambridge, UK, 1994.
3. C. Noguera, *Physics and Chemistry at Oxide Surfaces*, Cambridge University Press, Cambridge, UK, 1996.
4. A. R. José, F.-G. Marcos, *Synthesis, Properties, and Applications of Oxide Nanomaterials*, Willey, New Jersey, 2007.
5. G. Ertl, H. Knozinger, J. Weitkamp, *Handbook of Heterogeneous Catalysis*, Wiley-VHC, Weinheim, 1997.
6. J.-P. Jolivet, *Metal Oxide Chemistry and Synthesis: From Solution to Solid State*, Wiley, Chichester, 2000.
7. S. Iijima, *Helical microtubules of graphitic carbon*, Nature **354** (1991) 56-58.
8. G. R. Patzke, F. Krumeich, R. Nesper, *Oxidic nanotubes and nanorods - Anisotropic modules for a future nanotechnology*, Angew. Chem. Int. Ed. **41** (2002) 2446-2461.
9. Y. Y. Wu, H. Q. Yan, M. Huang, B. Messer, J. H. Song, P. D. Yang, *Inorganic semiconductor nanowires: Rational growth, assembly, and novel properties*, Chem. Eur. J. **8** (2002) 1261-1268.
10. C. N. R. Rao, F. L. Deepak, G. Gundiah, A. Govindaraj, *Inorganic nanowires*, Prog. Solid State Chem. **31** (2003) 5-147.
11. Z. R. Dai, Z. W. Pan, Z. L. Wang, *Novel nanostructures of functional oxides synthesized by thermal evaporation*, Adv. Func. Mater. **13** (2003) 9-24.
12. D. V. Bavykin, J. M. Friedrich, F. C. Walsh, *Protonated titanates and TiO_2 nanostructured materials: Synthesis, properties, and applications*, Adv. Mater. **18** (2006) 2807-2824.
13. C. N. R. Rao, A. Muller, A. K. Cheetham, *The Chemistry of Nanomaterials: Synthesis, Properties and Applications* Willey, Weinheim, 2004.
14. A. K. Bandyopadhyay, *Nano Materials: in Architecture, Interior Architecture and Design*, New Age International, New Delhi, 2008.
15. C. Nutzenadel, A. Zuttell, D. Chartouni, G. Schmid, L. Schlapbach, *Critical size and surface effect of the hydrogen interaction of palladium clusters*, Eur. Phys. J. D **8** (2000) 245-250.
16. G. C. Bond, C. Louis, D. T. Thompson, *Catalysis by Gold*, Imperial College Press, London, 2006.
17. J. Dutta, H. Hofmann, *Nanomaterials*, 2/11/05, [http://ltp2.epfl.ch/Cours/Nanomat/nanomat.pdf], 6/10/09.
18. I. Lee, F. Delbecq, R. Morales, M. A. Albiter, F. Zaera, *Tuning selectivity in catalysis by controlling particle shape*, Nat. Mater. **8** (2009) 132-138.

19. R. S. Feigelson, *Epitaxial growth of lithium niobate thin films by the solid source MOCVD method*, J. Cryst. Growth **166** (1996) 1-16.

20. L. Cot, A. Ayral, J. Durand, C. Guizard, N. Hovnanian, A. Julbe, A. Larbot, *Inorganic membranes and solid state sciences*, Solid State Sci. **2** (2000) 313-334.

21. R. Paily, A. DasGupta, N. DasGupta, P. Bhattacharya, P. Misra, T. Ganguli, L. M. Kukreja, A. K. Balamurugan, S. Rajagopalan, A. K. Tyagi, *Pulsed laser deposition of TiO$_2$ for MOS gate dielectric*, Appl. Phys. Lett. **187** (2002) 297-304.

22. M. B. Korzenski, P. Lecoeur, B. Mercey, D. Chippaux, B. Raveau, R. Desfeux, *PLD-grown Y$_2$O$_3$ thin films from Y metal: An advantageous alternative to films deposited from yttria*, Chem. Mater. **12** (2000) 3139-3150.

23. K. Byrappa, M. Haber, *Handbook of Hydrothermal Technology*, William Andrew, NY, 2001.

24. R. W. Goranson, *Solubility of Water in Granite Magmas*, Amer. J. Sci. **22** (1931) 481-502.

25. R. M. Barrer, *Syntheses and Reactions of Mordenite*, J. Chem. Soc. (1948) 2158-2163.

26. R. M. Barrer, *Molecular Sieves*, Soc. Chem. Ind., 1962.

27. S. Somiya, R. Roy, *Hydrothermal synthesis of fine oxide powders*, Bull. Mater. Sci. **23** (2000) 453-460.

28. S. Komarneni, H. Katsuki, *Nanophase materials by a novel microwave-hydrothermal process*, Pure Appl. Chem. **74** (2002) 1537-1543.

29. S. Komarneni, R. Roy, Q. H. Li, Microwave-hydrothermal synthesis of ceramic powders, Mater. Res. Bull. **27** (1992) 1393-1405.

30. T. Kasuga, M. Hiramatsu, A. Hoson, T. Sekino, K. Niihara, *Titania Nanotubes Prepared by Chemical Processing*, Adv. Mater. **11** (1999) 1307-1311.

31. T. Kasuga, M. Hiramatsu, A. Hoson, T. Sekino, K. Niihara, *Formation of Titanium Oxide Nanotube*, Langmuir **14** (1998) 3160-3163.

32. K. L. Berry, V. D. Aftandilian, W. W. Gilbert, E. P. H. Meibohm, H. S. Young, *Potassium tetra- and hexatitanates*, J. Inorg. Nucl. Chem. **14** (1960) 231.

33. T. Oota, H. Saito, *Synthesis of potassium hexatitanate fibers by the hydrothermal dehydration method*, J. Cryst. Growth **46** (1979) 331.

34. Y. Lan, X. P. Gao, H. Y. Zhu, Z. F. Zheng, T. Y. Yan, F. Wu, S. P. Ringer, D. Y. Song, *Titanate nanotubes and nanorods prepared from rutile powder*, Adv. Funct. Mater. **15** (2005) 1310-1318.

35. X. M. Sun, Y. D. Li, *Synthesis and characterization of ion-exchangeable titanate nanotubes*, Chem. Eur. J **9** (2003) 2229-2238.

36. G. K. L. Goh, F. F. Lange, S. M. Haile, C. G. Levi, *Hydrothermal synthesis of KNbO$_3$ and NaNbO$_3$ powders*, J. Mater. Res. **18** (2003) 338-345.

37. J. F. Liu, X. L. Li, Y. D. Li, *Synthesis and characterization of nanocrystalline niobates*, J. Cryst. Growth **247** (2003) 419-424.

38. I. Santos, L. H. Loureiro, M. F. P. Silva, A. M. V. Cavaleiro, *Studies on the hydrothermal synthesis of niobium oxides*, Polyhedron **21** (2002) 2009-2015.

39. S. Uchida, Y. Inoue, Y. Fujishiro, T. Sato, *Hydrothermal synthesis of $K_4Nb_6O_{17}$*, J. Mater. Sci. **33** (1998) 5125-5129.

40. F. Krumeich, H. J. Muhr, M. Niederberger, F. Bieri, B. Schnyder, R. Nesper, *Morphology and topochemical reactions of novel vanadium oxide nanotubes*, J. Am. Chem. Soc. **121** (1999) 8324-8331.

41. X. Wang, Y. D. Li, *Selected-control hydrothermal synthesis of alpha- and beta-MnO_2 single crystal nanowires*, J. Am. Chem. Soc. **124** (2002) 2880-2881.

42. G. R. Patzke, A. Michailovski, F. Krumeich, R. Nesper, J. D. Grunwaldt, A. Baiker, *One-step synthesis of submicrometer fibers of MoO_3*, Chem. Mater. **16** (2004) 1126-1134.

43. H. Y. Zhu, Y. Lan, X. P. Gao, S. P. Ringer, Z. F. Zheng, D. Y. Song, J. C. Zhao, *Phase transition between nanostructures of titanate and titanium dioxides via simple wet-chemical reactions*, J. Am. Chem. Soc. **127** (2005) 6730-6736.

44. Y. V. Kolen'ko, K. A. Kovnir, A. I. Gavrilov, A. V. Garshev, J. Frantti, O. I. Lebedev, B. R. Churagulov, G. Van Tendeloo, M. Yoshimura, *Hydrothermal synthesis and characterization of nanorods of various titanates and titanium dioxide*, J. Phys. Chem. B **110** (2006) 4030-4038.

45. X. B. Chen, S. S. Mao, *Titanium dioxide nanomaterials: Synthesis, properties, modifications, and applications*, Chem. Rev. **107** (2007) 2891-2959.

46. N. Miyamoto, K. Kuroda, M. Ogawa, *Exfoliation and film preparation of a layered titanate, $Na_2Ti_3O_7$, and intercalation of pseudoisocyanine dye*, J. Mater. Chem. **14** (2004) 165-170.

47. G. A. Somorjai, *Introduction to Surface Chemistry and Catalysis*, Wiley, NY, 1994.

48. U. Diebold, *The surface science of titanium dioxide*, Surface Science Reports **48** (2003) 53-229.

49. A. L. Linsebigler, G. Q. Lu, J. T. Yates, *Photocatalysis on TiO_2 Surfaces - Principles, Mechanisms, and Selected Results*, Chem. Rev. **95** (1995) 735-758.

50. K. L. Watters, R. F. Howe, T. P. Chojnacki, C.-M. Fu, R. L. Schneider, N.-B. Wong, *A chemical and physical characterization of alumina-supported $Rh_6(CO)_{16}$*, J. Catal. **66** (1980) 424-440.

51. G. Mirth, F. Eder, J. A. Lercher, *Design and application of a new reactor for in-situ infrared spectroscopic investigations of heterogenerously catalyzed-reacitons*, Applied Spectroscopy **48** (1994) 194-197.

52. D. H. Sullivan, W. C. Conner, M. P. Harold, *Surface-analysis with FT-IR emission specscopy*, Applied Spectroscopy **46** (1992) 811-818.

53. T. L. Thompson, J. T. Yates, *Surface science studies of the photoactivation of TiO_2-new photochemical processes*, Chem. Rev. **106** (2006) 4428-4453.

54. C. L. Thomas, *Catalytic Processes and Proven Catalysts*, Academic Press, New York, 1970.

55. J. M. Thomas, W. J. Thomas, *Principles and Practice of Heterogeneous Catalysis*, VCH, NY, 1996.

56. M. Haruta, S. Tsubota, T. Kobayashi, H. Kageyama, M. J. Genet, B. Delmon, *Low-Temperature Oxidation of Co over Gold Supported on TiO₂, Alpha-Fe₂O₃, and Co₃O₄*, J. Catal. **144** (1993) 175-192.

57. M. Haruta, N. Yamada, T. Kobayashi, S. Iijima, *Gold catalyst prepared by coprecipitation for low-temperature oxidations of hydrogen and of carbon monoxide*, J. Catal. **115** (1989) 301.

58. A. Arcadi, *Alternative synthetic methods through new developments in catalysis by gold*, Chem. Rev. **108** (2008) 3266-3325.

59. A. S. K. Hashmi, G. J. Hutchings, *Gold catalysis*, Angew. Chem. Int. Ed. **45** (2006) 7896-7936.

60. M. Valden, X. Lai, D. W. Goodman, *Onset of catalytic activity of gold clusters on titania with the appearance of nonmetallic properties*, Science **281** (1998) 1647-1650.

61. M. Haruta, *Size- and support-dependency in the catalysis of gold*, Catal. Today **36** (1997) 153-166.

62. R. Zanella, S. Giorgio, C. H. Shin, C. R. Henry, C. Louis, *Characterization and reactivity in CO oxidation of gold nanoparticles supported on TiO2 prepared by deposition-precipitation with NaOH and urea*, J. Catal. **222** (2004) 357-367.

63. R. Zanella, S. Giorgio, C. R. Henry, C. Louis, *Alternative methods for the preparation of gold nanoparticles supported on TiO₂*, J. Phys. Chem. B **106** (2002) 7634-7642.

64. J. M. C. Soares, P. Morrall, A. Crossley, P. Harris, M. Bowker, *Catalytic and noncatalytic CO oxidation on Au/TiO₂ catalysts*, J. Catal. **219** (2003) 17-24.

65. X. Y. Wang, S. P. Wang, S. R. Wang, Y. Q. Zhao, J. Huang, S. M. Zhang, W. P. Huang, S. H. Wu, *The preparation of Au/CeO₂ catalysts and their activities for low-temperature CO oxidation*, Catal. Lett. **112** (2006) 115-119.

66. S. Al-Sayari, A. F. Carley, S. H. Taylor, G. J. Hutchings, *Au/ZnO and Au/Fe₂O₃ catalysts for CO oxidation at ambient temperature: comments on the effect of synthesis conditions on the preparation of high activity catalysts prepared by coprecipitation*, Topics in Catal. **44** (2007) 123-128.

67. B. E. Solsona, T. Garcia, C. Jones, S. H. Taylor, A. F. Carley, G. J. Hutchings, *Supported gold catalysts for the total oxidation of alkanes and carbon monoxide*, Appl. Cata. A:General **312** (2006) 67-76.

68. M. Khoudiakov, M. C. Gupta, S. Deevi, *Au/Fe₂O₃ nanocatalysts for CO oxidation: A comparative study of deposition-precipitation and coprecipitation techniques*, Appl. Cata. A:General **291** (2005) 151-161.

69. A. M. Visco, F. Neri, G. Neri, A. Donato, C. Milone, S. Galvagno, *X-ray photoelectron spectroscopy of Au/Fe₂O₃ catalysts*, Phys. Chem. Chem. Phys. **1** (1999) 2869-2873.

70. H. H. Kim, S. Tsubota, M. Date, A. Ogata, S. Futamura, *Catalyst regeneration and activity enhancement of Au/TiO₂ by atmospheric pressure nonthermal plasma*, Appl. Cata. A:General **329** (2007) 93-98.

71. W. C. Li, M. Comotti, F. Schuth, *Highly reproducible syntheses of active*

Au/TiO$_2$ catalysts for CO oxidation by deposition-precipitation or impregnation, J. Catal. **237** (2006) 190-196.

72. S. H. Wu, X. C. Zheng, S. R. Wang, D. Z. Han, W. P. Huang, S. M. Zhang, *TiO$_2$ supported nano-Au catalysts prepared via solvated metal atom impregnation for low-temperature CO oxidation*, Catal. Lett. **96** (2004) 49-55.

73. B. L. Zhu, K. R. Li, Y. F. Feng, S. M. Zhang, S. H. Wu, W. P. Huang, *Synthesis and catalytic performance of gold-loaded TiO$_2$ nanofibers*, Catal. Lett. **118** (2007) 55-58.

74. B. L. Zhu, Q. Guo, X. L. Huang, S. R. Wang, S. M. Zhang, S. H. Wu, W. P. Huang, *Characterization and catalytic performance of TiO$_2$ nanotubes-supported gold and copper particles*, J. Mol. Cat. A: Chem. **249** (2006) 211-217.

75. G. C. Bond, D. T. Thompson, *Gold-catalysed oxidation of carbon monoxide*, Gold Bull. **33** (2000) 41-51.

76. C. K. Costello, J. H. Yang, H. Y. Law, Y. Wang, J. N. Lin, L. D. Marks, M. C. Kung, H. H. Kung, *On the potential role of hydroxyl groups in CO oxidation over Au/Al$_2$O$_3$*, Appl. Catal. A **243** (2003) 15-24.

77. M. Date, M. Okumura, S. Tsubota, M. Haruta, *Vital role of moisture in the catalytic activity of supported gold nanoparticles*, Angew. Chem. Int. Ed. **43** (2004) 2129-2132.

78. Z. Y. Zhong, J. Highfield, M. Lin, J. Teo, Y. F. Han, *Insights into the oxidation and decomposition of CO on Au/alpha-Fe$_2$O$_3$ and on alpha-Fe$_2$O$_3$ by coupled TG-FTIR*, Langmuir **24** (2008) 8576-8582.

79. M. Haruta, *Catalysis - Gold rush*, Nature **437** (2005) 1098-1099.

80. M. C. Kung, R. J. Davis, H. H. Kung, *Understanding Au-catalyzed low-temperature CO oxidation*, J. Phys. Chem. C **111** (2007) 11767-11775.

81. A. Vittadini, A. Selloni, F. P. Rotzinger, M. Grätzel, *Structure and energetics of water adsorbed at TiO$_2$ anatase (101) and (001) surfaces*, Phys. Rev. Lett. **81** (1998) 2954-2957.

82. L. M. Liu, B. McAllister, H. Q. Ye, P. Hu, *Identifying an O$_2$ supply pathway in CO oxidation on Au/TiO$_2$(110): A density functional theory study on the intrinsic role of water*, J. Am. Chem. Soc. **128** (2006) 4017-4022.

83. M. A. Henderson, W. S. Epling, C. H. F. Peden, C. L. Perkins, *Insights into Photoexcited Electron Scavenging Processes on TiO$_2$ Obtained from Studies of the Reaction of O$_2$ with OH Groups Adsorbed at Electronic Defects on TiO$_2$(110)*, J Phys. Chem. B **107** (2003) 534-545.

84. M. Grätzel, *Photoelectrochemical cells*, Nature **414** (2001) 338-344.

85. A. Fujishima, K. Hongda, *Electrochemical photolysis of water at a semiconductor electrode*, Nature **238** (1972) 37-38.

86. M. Ni, M. K. H. Leung, D. Y. C. Leung, K. Sumathy, *A review and recent developments in photocatalytic water-splitting using TiO$_2$ for hydrogen production*, Renew. Sust. Energy Rev. **11** (2007) 401-425.

87. Z. G. Zou, J. H. Ye, K. Sayama, H. Arakawa, *Direct splitting of water under visible light irradiation with an oxide semiconductor photocatalyst*, Nature

414 (2001) 625-627.

88.   K. Koci, L. Obalova, L. Matejova, D. Placha, Z. Lacny, J. Jirkovsky, O. Solcova, *Effect of TiO$_2$ particle size on the photocatalytic reduction of CO$_2$*, Appl. Catal. B **89** (2009) 494-502.

89.   H. Yamashita, H. Nishiguchi, N. Kamada, M. Anpo, Y. Teraoka, H. Hatano, S. Ehara, K. Kikui, L. Palmisano, A. Sclafani, M. Schiavello, M. A. Fox, *Photocatalytic reductionof CO$_2$ with H$_2$O on TiO$_2$ and Cu/TiO$_2$ catalysts*, Res. Chem. Intermed. **20** (1994) 815-823.

90.   M. R. Hoffmann, S. T. Martin, W. Y. Choi, D. W. Bahnemann, *Environmental Applications of Semiconductor Photocatalysis*, Chemical Reviews **95** (1995) 69-96.

91.   M. I. Litter, *Heterogeneous photocatalysis - Transition metal ions in photocatalytic systems*, Appl. Catal. B **23** (1999) 89-114.

92.   M. A. Fox, M. T. Dulay, *Heterogeneous Photocatalysis*, Chem. Rev. **93** (1993) 341-357.

93.   A. Wold, *Photocatalytic properties of TiO$_2$*, Chem. Mater. **5** (1993) 280-283.

94.   M. R. Hoffmann, S. T. Martin, W. Y. Choi, D. W. Bahnemann, *Environmental Applications of Semiconductor Photocatalysis*, Chem. Rev. **95** (1995) 69-96.

95.   S. Bakardjieva, V. Stengl, L. Szatmary, J. Subrt, J. Lukac, N. Murafa, D. Niznansky, K. Cizek, J. Jirkovsky, N. Petrova, *Transformation of brookite-type TiO$_2$ nanocrystals to rutile: correlation between microstructure and photoactivity*, J. Mater. Chem. **16** (2006) 1709-1716.

96.   R. L. Penn, J. F. Banfield, *Formation of rutile nuclei at anatase {112} twin interfaces and the phase transformation mechanism in nanocrystalline titania*, Am. Mineral. **84** (1999) 871-876.

97.   R. Marchand, L. Brohan, M. Tournoux, *TiO$_2$(B) a new form of titanium dioxide and the potassium octatitanate K$_2$Ti$_8$O$_{17}$*, Mater. Res. Bull. **15** (1980) 1129-1133.

98.   M. Tournoux, R. Marchand, L. Brohan, *Layered K$_2$Ti$_4$O$_9$ and the open metastable TiO$_2$(B) structure*, Prog. Solid State Chem. **17** (1986) 33-52.

99.   L. R. Wallenberg, M. Sanati, A. Andersson, *A high-resolution electron microscopy investigation of TiO$_2$(B)-supported vanadium oxide catalysts*, J. Catal. **126** (1990) 246-260.

100.   T. P. Feist, P. K. Davies, *The Soft Chemical Synthesis of TiO$_2$ (B) from Layered Titanates*, J. Solid State Chem. **101** (1992) 275-295.

101.   T. Kogure, T. Umezawa, Y. Kotani, A. Matsuda, M. Tatsumisago, T. Minami, *Formation of TiO$_2$(B) nanocrystallites in sol-gel-derived SiO$_2$-TiO$_2$ film*, J. Am. Ceram. Soc. **82** (1999) 3248-3250.

102.   J. F. Banfield, D. R. Veblen, D. J. Smith, *The identification of naturally occurring TiO$_2$ (B) by structure determination using high resolution electron microscopy, image simulation, and distance-least-squares refinement*, Am. Mineral. **76** (1991) 343.

103.   G. Guisbiers, O. Van Overschelde, M. Wautelet, *Theoretical investigation of size and shape effects on the melting temperature and energy bandgap of TiO$_2$*

nanostructures, Appl. Phys. Lett. **92** (2008).

104. K. Tanaka, M. F. V. Capule, T. Hisanaga, *Effect of crystallinity of TiO₂ on its photocatalytic action*, Chem. Phys. Lett. **187** (1991) 73-76.

105. K. Yanagisawa, J. Ovenstone, *Crystallization of anatase from amorphous titania using the hydrothermal technique: Effects of starting material and temperature*, J. Phys. Chem. B **103** (1999) 7781-7787.

106. D. C. Hurum, K. A. Gray, T. Rajh, M. C. Thurnauer, *Recombination Pathways in the Degussa P25 Formulation of TiO₂: Surface versus Lattice Mechanisms*, J. Phys. Chem. B **109** (2005) 977-980.

107. S. Yin, J. H. Wu, M. Aki, T. Sato, *Photocatalytic hydrogen evolution with fibrous titania prepared by the solvothermal reactions of protonic layered tetratitanate (H₂Ti₄O₉)*, Int. J. Inorg. Mater. **2** (2000) 325-331.

108. G. Betz, H. Tributsch, R. Marchand, *Hydrogen insertion (intercalation) and light induced proton exchange at TiO₂(B) -electrodes*, J. Appl. Electrochem. **14** (1984) 315-322.

109. H. Verweij, *Ceramic membranes: Morphology and transport*, J. Mater. Sci. **38** (2003) 4677-4695.

110. R. M. de Vos, H. Verweij, *High-selectivity, high-flux silica membranes for gas separation*, Science **279** (1998) 1710-1711.

111. A. I. Schaefer, A. G. Fane, T. D. Waite, *NanofiltrationaPrinciples and Applications*, Elsevier, Oxford, 2003.

112. R. R. Bhave, *Inorganic Membranes: Synthesis, Characterisation and Applications*, Van Nostrand Reinhold, New York, 1991.

113. R. W. Baker, *Membrane Technology and Applications, 2nd ed*, Wiley, Chichester, UK, 2004.

114. S. P. Nunes, M. L. Sforca, K. V. Peinemann, *Dense Hydrophilic Composite Membranes for Ultrafiltration*, J. Membr. Sci. **106** (1995) 49-56.

115. H. Y. Zhu, X. P. Gao, Y. Lan, D. Y. Song, Y. X. Xi, J. C. Zhao, *Hydrogen titanate nanofibers covered with anatase nanocrystals: A delicate structure achieved by the wet chemistry reaction of the titanate nanofibers*, J. Am. Chem. Soc. **126** (2004) 8380-8381.

116. M. Nyman, F. Bonhomme, T. M. Alam, M. A. Rodriguez, B. R. Cherry, J. L. Krumhansl, T. M. Nenoff, A. M. Sattler, *A general synthetic procedure for heteropolyniobates*, Science **297** (2002) 996-998.

117. C. H. An, K. B. Tang, C. R. Wang, G. Z. Shen, Y. Jin, Y. T. Qian, *Characterization of LiNbO₃ nanocrystals prepared via a convenient hydrothermal route*, Mater. Res. Bull. **37** (2002) 1791-1796.

118. K. Domen, A. Kudo, M. Shibata, A. Tanaka, K.-I. Maruya, T. Onishi, *Novel photocatalysts, ion-exchanged K₄Nb₆O₁₇, with a layer structure*, J. Chem. Soc., Chem. Commun (1986) 1706 - 1707.

119. H. J. Qiao, J. J. Xu, G. Q. Zhang, X. Z. Zhang, Q. Sun, G. Y. Zhang, *Ultraviolet photorefractivity features in doped lithium niobate crystals*, Phys. Rev. B **70** (2004).

120. Y. Saito, H. Takao, T. Tani, T. Nonoyama, K. Takatori, T. Homma, T. Nagaya,

M. Nakamura, *Lead-free piezoceramics*, Nature **432** (2004) 84-87.

121. E. R. Camargo, M. Popa, M. Kakihana, *Sodium niobate (NaNbO₃) powders synthesized by a wet-chemical method using a water-soluble malic acid complex*, Chem. Mater. **14** (2002) 2365-2368.

122. H. W. Xu, M. Nyman, T. M. Nenoff, A. Navrotsky, *Prototype sandia octahedral molecular sieve (SOMS) Na₂Nb₂O₆-H₂O: Synthesis, structure and thermodynamic stability*, Chem. Mater. **16** (2004) 2034-2040.

123. A. Nazeri-Eshghi, A. X. Kuang, J. D. Mackenzie, *Preparation and properties of KNbO₃ via the sol-gel method*, J. Mater. Sci. **25** (1990) 3333.

124. M. Nyman, A. Tripathi, J. B. Parise, R. S. Maxwell, T. M. Nenoff, *Sandia octahedral molecular sieves (SOMS): Structural and property effects of charge-balancing the M-IV-substituted (M = Ti, Zr) niobate framework*, J. Am. Chem. Soc. **124** (2002) 1704-1713.

125. M. A. L. Nobre, E. Longo, E. R. Leite, J. A. Varela, *Synthesis and sintering of ultra fine NaNbO₃ powder by use of polymeric precursors*, Mater. Lett. **28** (1996) 215-220.

126. M. Nyman, A. Tripathi, J. B. Parise, R. S. Maxwell, W. T. A. Harrison, T. M. Nenoff, *A new family of octahedral molecular sieves: Sodium Ti/Zr-IV niobates*, J. Am. Chem. Soc. **123** (2001) 1529-1530.

127. C. R. Cho, I. Katardjiev, M. Grishin, A. Grishin, *Na₀.₅K₀.₅NbO₃ thin films for voltage controlled acoustoelectric device applications*, Appl. Phys. Lett. **80** (2002) 3171-3173.

128. G. S. Maciel, N. Rakov, C. B. de Araujo, A. A. Lipovskii, D. K. Tagantsev, *Optical limiting behavior of a glass-ceramic containing sodium niobate crystallites*, Appl. Phys. Lett. **79** (2001) 584-586.

129. J. F. Zhu, J. L. Zhang, F. Chen, M. Anpo, *Preparation of high photocatalytic activity TiO₂ with a bicrystalline phase containing anatase and TiO₂ (B)*, Mater. Lett. **59** (2005) 3378-3381.

130. H. L. Kuo, C. Y. Kuo, C. H. Liu, J. H. Chao, C. H. Lin, *A highly active bi-crystalline photocatalyst consisting of TiO₂ (B) nanotube and anatase particle for producing H₂ gas from neat ethanol*, Catal. Lett. **113** (2007) 7-12.

131. A. Nardelli, (2008) *Photoabsorption of gold nanoparticles: a TDDFT analysis by cluster model molecule*, PhD thesis, University of Trieste.

132. E. A. Behrens, P. Sylvester, A. Clearfield, *Assessment of a sodium nonatitanate and pharmacosiderite-type ion exchangers for strontium and cesium removal from DOE waste simulants*, Environ. Sci. Technol. **32** (1998) 101-107.

133. G. M. Bancroft, J. B. Metson, S. M. Kanetkar, J. D. Brown, *Surface studies on a leached sphene glass*, Nature **299** (1982) 708.

134. D. H. Sun, C. Chang, S. Li, L. W. Lin, *Near-field electrospinning*, Nano Lett. **6** (2006) 839-842.

135. P. Katta, M. Alessandro, R. D. Ramsier, G. G. Chase, *Continuous electrospinning of aligned polymer nanofibers onto a wire drum collector*, Nano Lett. **4** (2004) 2215-2218.

136. A. G. MacDiarmid, *"Synthetic metals": A novel role for organic polymers (Nobel lecture)*, Angew. Chem. Int. Ed. **40** (2001) 2581-2590.

137. M. G. McKee, J. M. Layman, M. P. Cashion, T. E. Long, *Phospholipid nonwoven electrospun membranes*, Science **311** (2006) 353-355.

138. F. Tepper, T. Rivkin, G. Lukasic, *Novel nanofibre filter medium attracts waterborne pathogens*, Filtr. Sep. **39** (2002) 16-19.

139. P. K. Kang, D. O. Shah, *Filtration of nanoparticles with dimethyldioctadecylammonium bromide treated microporous polypropylene filters*, Langmuir **13** (1997) 1820-1826.

140. S. Y. Yang, I. Ryu, H. Y. Kim, J. K. Kim, S. K. Jang, T. P. Russell, *Nanoporous membranes with ultrahigh selectivity and flux for the filtration of viruses*, Adv. Mater. **18** (2006) 709-712.

141. T. Harper, C. R. Vas, P. Holister, *Feeling the chemical industry's future*, Chem. Eng. Prog. **99** (2003) 34S-38S.